Since January 2020 Elsevier has created a COVID-19 resource centre with free information in English and Mandarin on the novel coronavirus COVID-19. The COVID-19 resource centre is hosted on Elsevier Connect, the company's public news and information website.

Journal of Molecular Liquids 363 (2022) 119878

Contents lists available at ScienceDirect

Journal of Molecular Liquids

journal homepage: www.elsevier.com/locate/molliq

Charge-transfer chemistry of two corticosteroids used adjunctively to treat COVID-19. Part II: The CT reaction of hydrocortisone and dexamethasone donors with TCNQ and fluoranil acceptors in five organic solvents

Moamen S. Refat [a], Bander Albogami [b], Abdel Majid A. Adam [a,*], Hosam A. Saad [a], Amnah Mohammed Alsuhaibani [c], Lal Miyan [d], Mohamed S. Hegab [e]

[a] Department of Chemistry, College of Science, Taif University, P.O. Box 11099, Taif 21944, Saudi Arabia
[b] Department of Biology, College of Science, Taif University, P.O. Box 11099, Taif 21944, Saudi Arabia
[c] Department of Physical Sport Science, College of Education, Princess Nourah bint Abdulrahman University, P.O. Box 84428, Riyadh 11671, Saudi Arabia
[d] Department of Chemistry, Faculty of Science, Aligarh Muslim University, Aligarh 202002(UP), India
[e] Deanship of Supportive Studies (D.S.S.), Taif University, P.O. Box 11099, Taif 21944, Saudi Arabia

ARTICLE INFO

Article history:
Received 8 June 2022
Revised 4 July 2022
Accepted 15 July 2022
Available online 21 July 2022

Keywords:
Dexamethasone
Hydrocortisone
Charge-transfer interaction
TCNQ acceptor
TFQ acceptor
Organic solvents

ABSTRACT

Hydrocortisone (termed as D1) and dexamethasone (termed as D2) are corticosteroids currently used to treat COVID-19. COVID-19 is a disease caused by severe acute respiratory syndrome coronavirus 2 (SARS-CoV-2). Exploring additional chemical properties of drugs used in the treatment protocols for COVID-19 could help scientists alike improve these treatment protocols and potentially even the vaccines (i.e., Janssen, Moderna, AstraZeneca, Pfizer-BioNTech). In this work, the charge-transfer (CT) properties of these two corticosteroids (D1 and D2) with two universal acceptors: 7,8,8-tetracyanoquinodimethane (termed as TCNQ) and fluoranil (termed as TFQ) in five different solvents were investigated. The examined solvents were MeOH, EtOH, MeCN, CH_2Cl_2, and $CHCl_3$. The CT interactions formed stable corticosteroid CT complexes in all examined solvents. Several spectroscopic parameters were derived, and the oscillator strength (*f*) and transition dipole moment ($\mu_{e.g.}$) values revealed that the interaction between the investigated corticosteroids with TCNQ acceptor is much stronger than their interaction with TFQ acceptor. The CT interactions were proposed to process via n → π* transition.

1. Introduction

On December 9, 2019, a novel coronavirus (severe acute respiratory syndrome coronavirus 2, SARS-CoV-2) originated from a seafood market in Wuhan, China, rapidly becoming a destabilizing global pandemic. By early March 2020, after the SARS-CoV-2 outbreak had affected millions worldwide, the World Health Organization (WHO) termed the acute respiratory syndrome resulting from SARS-CoV-2 infection the COronaVIrus Disease 2019 (COVID-19) and declared it a pandemic [1–3], become the biggest outbreak that the world ever seen [4]. COVID-19 has killed more than 6.15 million and infected more than 490 million people worldwide (as of April 1, 2022) [5]. Several pharmacological approaches have been implemented based on previous experience and evidence from prior outbreaks of respiratory-targeting viruses, such as SARS-CoV in China in 2003 and the MERS-CoV in the Middle East in 2012 [6,7]. These therapeutic approaches include corticosteroids, tocilizumab, azithromycin, lopinavir/ritonavir, remdesivir, chloroquine, and hydroxychloroquine. For more than 70 years, corticosteroids have been used in the treatment of inflammatory diseases, and oral infections due to their strong immunomodulatory and anti-inflammatory properties; in general, corticosteroids modulate the immune response to treat a wide variety of diseases by preventing and attenuating inflammation [8,9]. Corticosteroids are widely used adjunctively to treat critically ill patients with COVID-19 because they reduce inflammation-induced lung injury by suppressing lung inflammation [10–14]. Corticosteroids decrease patients' dependency on mechanical ventilation, the duration of shock on circulatory support, the length of intensive care unit (ICU) stays, and potentially even mortality.

11β,17α,21-trihydroxypregn-4-ene-3,20-dione (hydrocortisone) and 9α-fluoro-16α-methyl-11β,17α,21-trihydroxy-1,4-preg

* Corresponding author.
E-mail address: majidadam@tu.edu.sa (A.M.A. Adam).

https://doi.org/10.1016/j.molliq.2022.119878
0167-7322/

nadiene-3,20-dione (dexamethasone), their chemical structures are shown in Fig. 1, are the most widely used corticosteroids in the treatment of COVID-19. Dexamethasone and hydrocortisone possess strong anti-inflammatory properties and treat severe skin allergies and inflammation, but dexamethasone has potent anti-inflammatory effects more than hydrocortisone by 25–50 times [15,16]. Because of that, dexamethasone is well suited for short-term use in acute and severe inflammatory cases and is also used to treat aphthous stomatitis, vesicular stomatitis, and ulcers. It inhibits the production of new immune cells and the formation of prostaglandins (pro-inflammatory substances), thereby suppressing the amplification of immune reactions [17–19].

Charge transfer (CT) or donor-acceptor complexations are interactions that involve transferring an electronically charged particle between two molecules, the one that donates the charge is commonly known as the electron-donating (donor; D) molecule, whereas the one that accepts the charge is commonly known as electron-accepting (acceptor; A) molecule. The transferring could be symbolized as (D → A), and the generated complex by this interaction could be formulated as $[D^{+\cdot} A^{-\cdot}]$ [20–27]. After Robert Mulliken introduced the concept of CT interaction in 1969, Roy Foster widely disseminated it, and since then, it has become well established that CT interactions involve the formation of a weak bond combined with a great color change. The strong color changes used to identify the resultant CT complex reflect a change in the UV/Vis spectrum of D and/or A molecules appearing in the form of either a new absorption band that did not exist in the spectra of the D and A molecules or increasing of the intensity of the already existing UV/Vis bands.

CT interactions researchers noted that the generated products possess unique chemical, physical, and biological properties via this type of interaction. Beneficiations of CT interactions are not limited to basic sciences (biology, biochemistry, chemistry, physics) but extended to applied sciences (medicine, pharmacology, technology, industry, material science, engineering) [21,28–86]. In the past years, we have been interested in examining the CT behavior of numerous biologically active donor molecules by reacting them with different organic and inorganic accepting molecules in different media [87–121]. Since the onset of the SARS-CoV-2 pandemic, we shifted our focus from biologically active donor molecules to the CT properties of the pharmacological agents used to combat COVID-19 and their modifiability. We think obtaining new insights into the CT behavior of active compounds used in the treatments for COVID-19 will provide insight into the mechanisms underlying their effective properties and can help scientists alike to optimize and improve these treatment protocols and potentially even the vaccines (Janssen, Moderna, AstraZeneca, Pfizer-BioNTech). In a four-part work, we pioneered this new research effort with a comprehensive investigation into the CT chemistry of azithromycin, an antibiotic widely used in the treatment of COVID-19 [34–37].

As a continuation of these works, our newest series aims to furnish a big-picture perspective on the CT property of hydrocortisone and dexamethasone, corticosteroids widely used in the treatment of COVID-19. In part I [122], we described the CT interactions of these two corticosteroids with the 2,3-dichloro-5,6-dicyano-*p*-benzoquinone acceptor. In the current part of the work (Part II), we described the CT interactions of hydrocortisone and dexamethasone with two new accepting-molecules, 7,7,8,8-tetracyano quinodimethane (termed as TCNQ) and fluoranil (termed as TFQ) (Fig. 2) in five organic solvents.

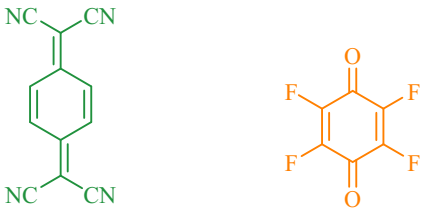

Fig. 2. Chemical structures of the used accepting-molecules (TCNQ and TFQ).

2. Experimental

2.1. Reagents and solvents

The used solvents in this study: MeOH, EtOH, MeCN, CH_2Cl_2, and $CHCl_3$ were spectroscopic-grade solvents and obtained from Fluka (Lausanne, Switzerland). The investigated organic acceptors supplied by the Merck KGaA (Darmstadt, Germany) were 7,7,8,8-tetracyanoquinodimethane (TCNQ) and fluoranil (TFQ). The examined donors obtained from Sigma-Aldrich (Saint Louis, MO, USA) were hydrocortisone (abbreviated here as D1) and hydrocortisone (abbreviated here as D2). All the donors and acceptors were obtained from the commercial sources at the highest purity available, which were ≥ 98 % HPLC for D1, 99 % HPLC for D2, 98 % for TCNQ, and 97 % for TFQ.

2.2. Analytical

2.2.1. UV/Visible spectra

The UV/Visible spectrophotometry was applied to collect the UV/Visible spectra of the D1 and D2 soluble complexes with TCNQ and TFQ acceptors in the investigated solvents. These electronic spectra were helpful for:

(i) Characterization of the CT phenomena between the donors (D1 and D2) and the acceptors (TCNQ and TFQ) in different solvents.
(ii) Identification of the charge transfer (CT) electronic absorption band that characterize the D1-TCNQ, D2-TCNQ, D1-TFQ, and D2-TFQ soluble complex in each solvent.

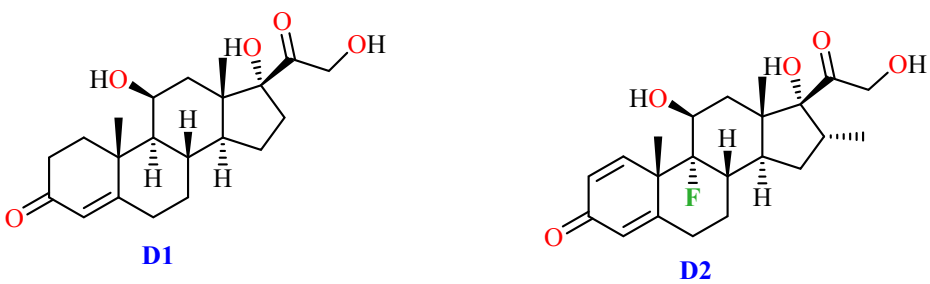

Fig. 1. Chemical structures of hydrocortisone (D1) and dexamethasone (D2).

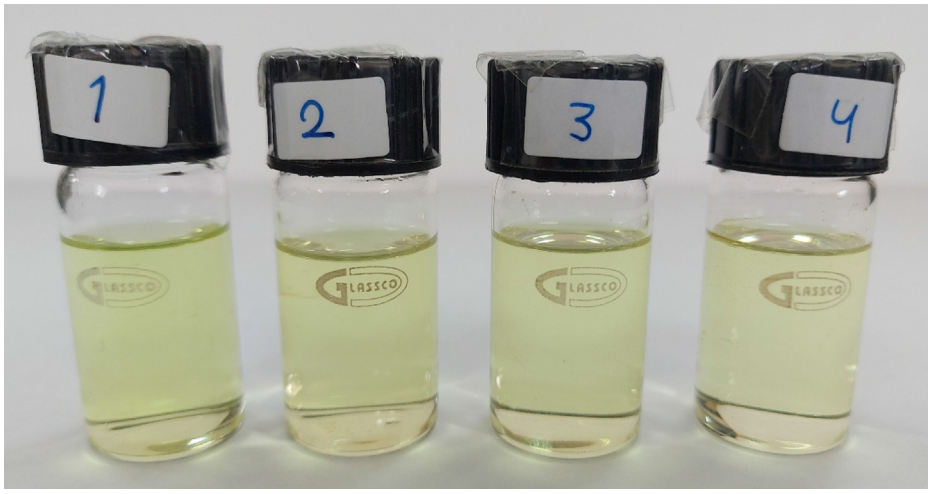

Fig. 3. Color of the TCNQ solution in the MeOH (1), MeCN (2), CH_2Cl_2 (4), and $CHCl_3$ (5) solvents.

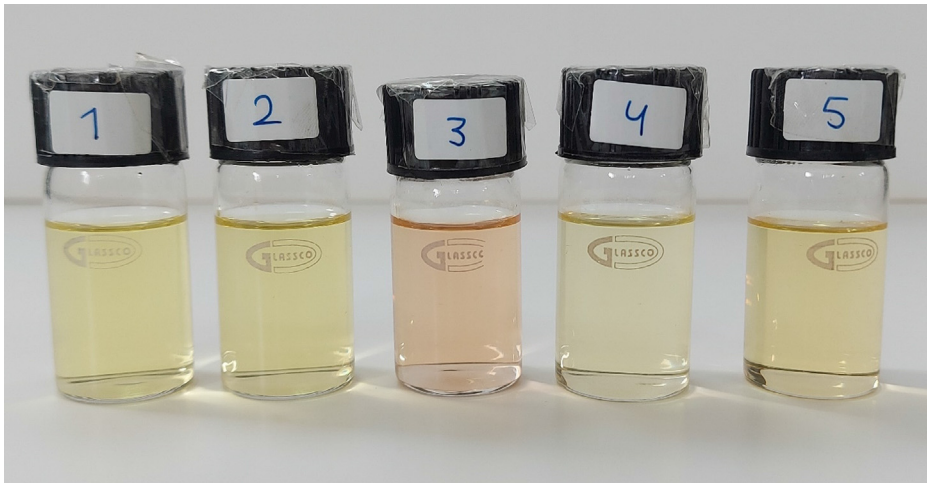

Fig. 4. Color of the TFQ solution in the MeOH (1), EtOH (2), MeCN (3), CH_2Cl_2 (4), and $CHCl_3$ (5) solvents.

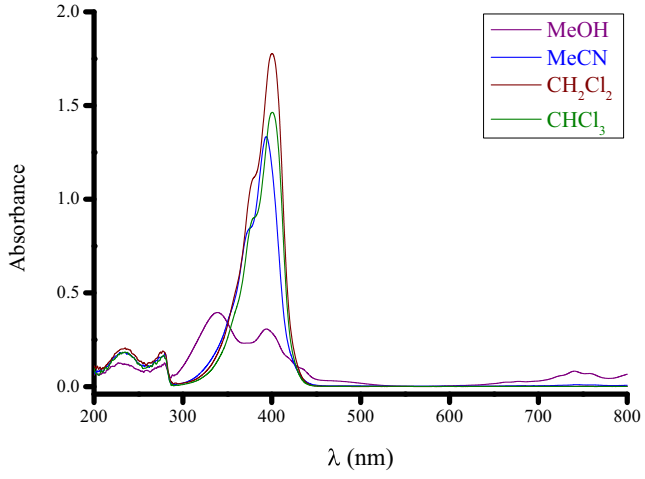

Fig. 5. The UV/Vis spectra of the TCNQ acceptor in the MeOH, MeCN, CH_2Cl_2, and $CHCl_3$ solvents.

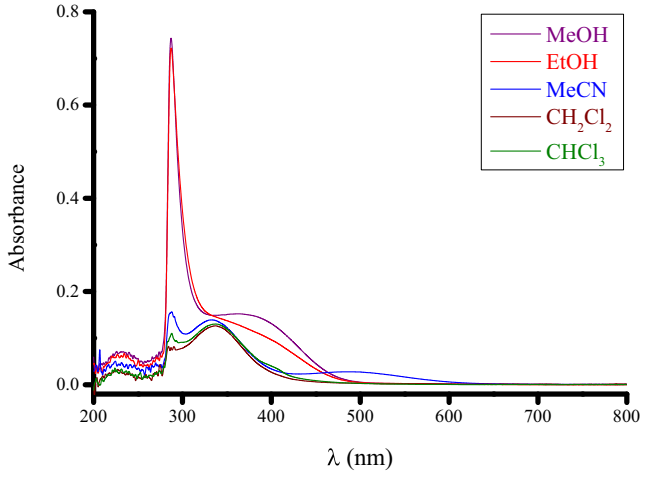

Fig. 6. The UV/Vis spectra of the TFQ acceptor in the MeOH, EtOH, MeCN, CH_2Cl_2, and $CHCl_3$ solvents.

(iii) Verify the wavelength (in nm) corresponding to the CT electronic absorption band (λ_{CT}) for all soluble CT complexes.

To obtain the UV/Visible spectra, first, standard solutions of D1, D2, TCNQ, and TFQ were prepared in a specific solvent (MeOH, EtOH, MeCN, CH_2Cl_2, and $CHCl_3$) (5×10^{-4} M). Second, the D1-TCNQ, D2-TCNQ, D1-TFQ, and D2-TFQ systems in each solvent were prepared by mixing equal amounts (1 mL) of the donor and acceptor standard solutions in a 5 mL volumetric flask and completing the volume up to the mark by the solvent. Finally, all the prepared systems were scanned using a Cary 7000 UV–vis–NIR Spectrophotometer from Agilent Technologies, Australia, in the 200–800 nm region. The electronic features of each CT system were obtained by comparing the UV/Visible spectra of the systems with those of the corresponding free components (D1, D2, TCNQ, and TFQ).

2.2.2. Infrared (IR) spectra

The IR spectrophotometry was applied to obtain the IR spectra of the D1 and D2 solid CT complexes with the acceptors in the investigated solvents. Observing and analyzing the IR spectra of the formed CT complexes were helpful for:

i) Observing the changes in the characteristic IR spectral bands of free reactants after the complexation process.

Table 1
Wavelengths (in nm) of the characteristic absorption bands appear of TCNQ and TFQ acceptors in MeOH, EtOH, MeCN, $CHCl_3$, and CH_2Cl_2 solvents alongside the corresponding CT complexes.

Compound	Wavelength of the characteristic absorption bands (nm)					
	UV			Vis		
	MeOH, EtOH	MeCN	CH_2Cl_2, $CHCl_3$	MeOH, EtOH	MeCN	CH_2Cl_2, $CHCl_3$
TCNQ acceptor	339	–	–	394	394	400
TFQ acceptor	287	333	337	362, 340	487	–
D1–TCNQ complex	343	–	–	394	394	400
D2–TCNQ complex	342	–	–	394	394	400
D1–TFQ complex	289	333	337	362, 340	487	–
D2–TFQ complex	289	333	337	362, 340	487	–

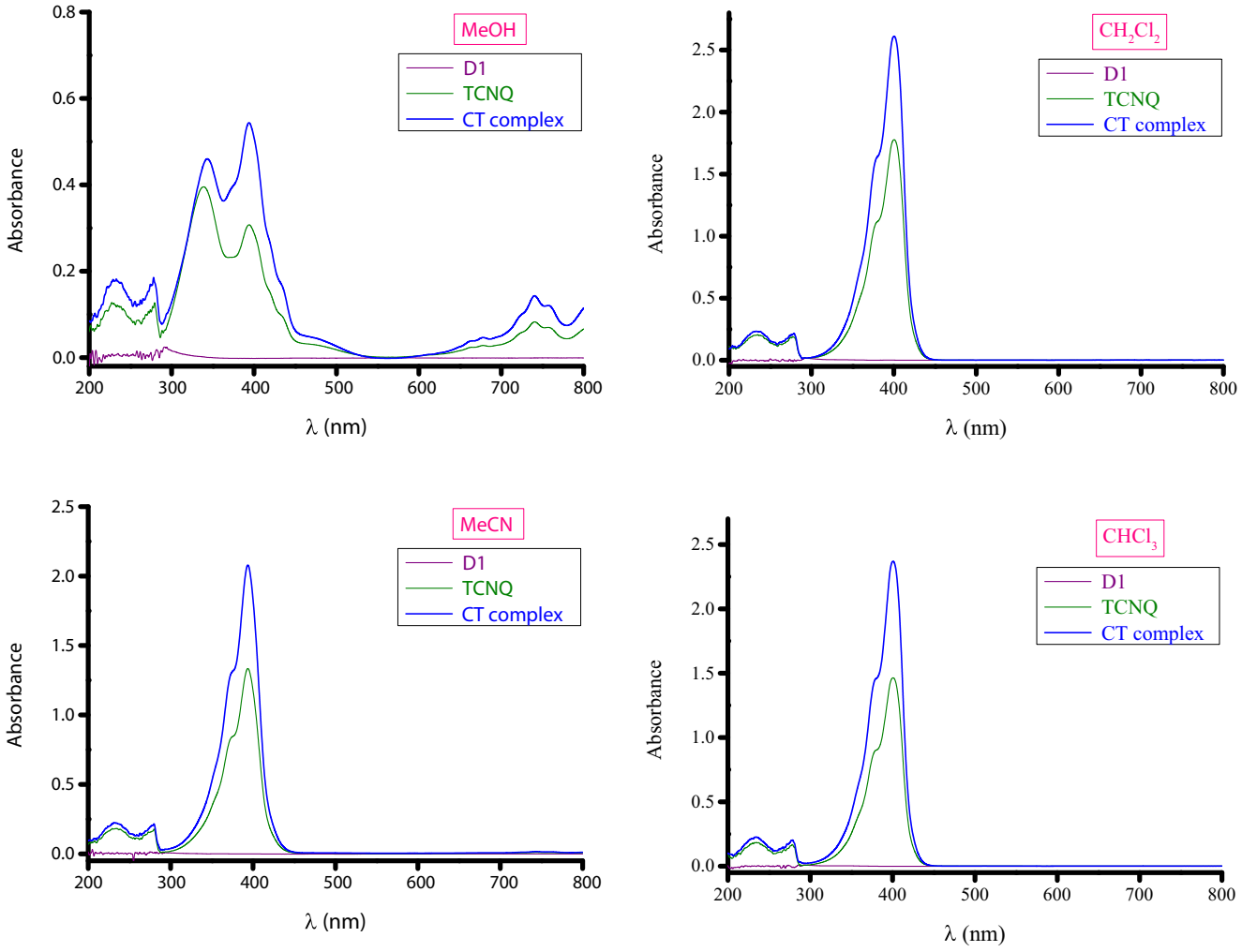

Fig. 7. The UV/Vis spectra of the D1–TCNQ complex in MeOH, MeCN, CH_2Cl_2, and $CHCl_3$ solvents alongside with their free reactants.

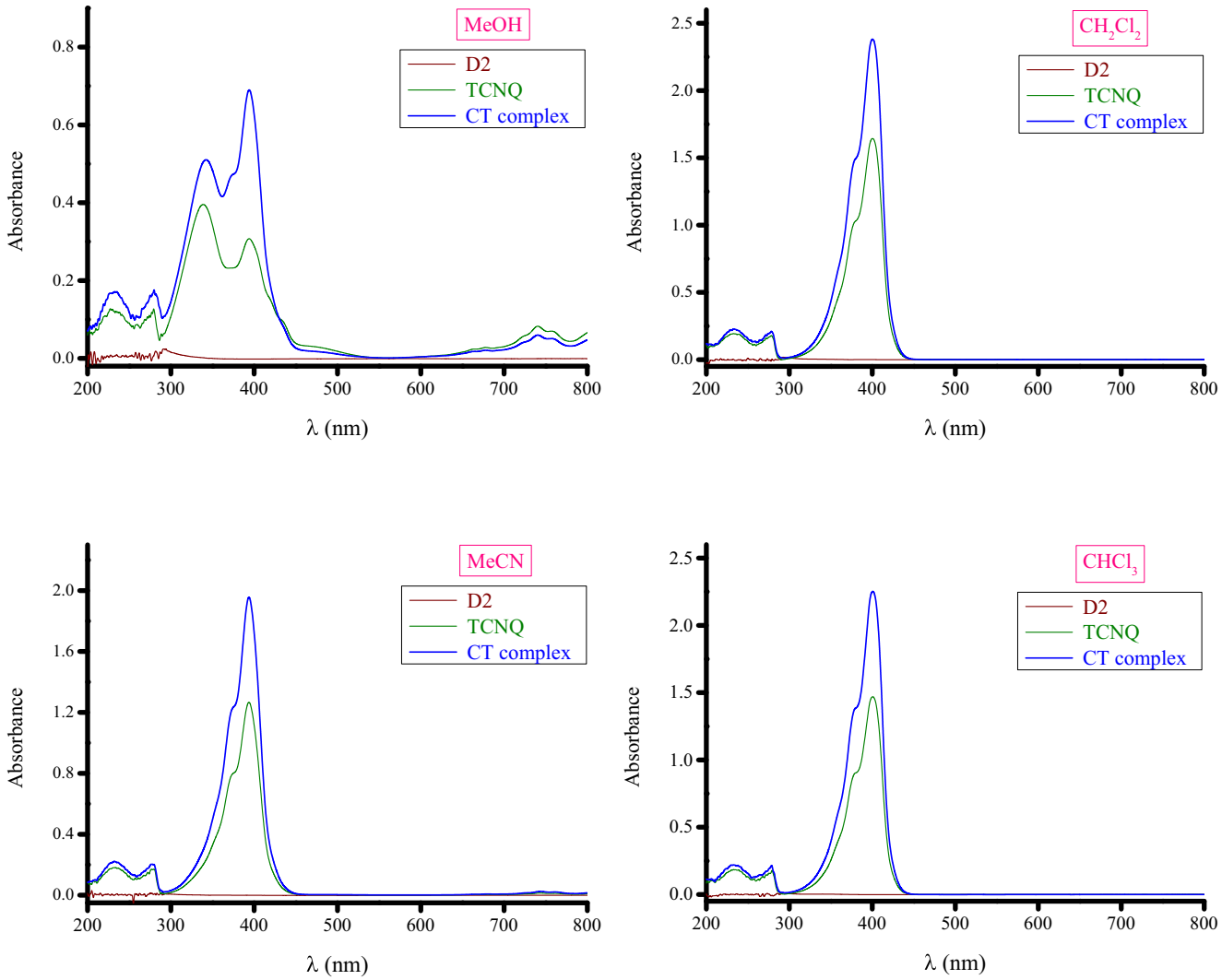

Fig. 8. The UV/Vis spectra of the D1–TCNQ complex in MeOH, MeCN, CH_2Cl_2, and $CHCl_3$ solvents alongside with their free reactants.

ii) Confirming the CT interaction between D1 and D2 with TCNQ and TFQ acceptors in each solvent.
iii) Proposing the suitable mechanisms of the investigated CT interactions.

To obtain the IR spectra, concentrated solutions of D1, D2, TCNQ, and TFQ (2 mmol in 20 mL solvent) were prepared in a specific solvent (MeOH, EtOH, MeCN, CH_2Cl_2, and $CHCl_3$). Second, the concentrated D1 and D2 solutions were mixed with the corresponding acceptor concentrated solution to generate the D1-TCNQ, D2-TCNQ, D1-TFQ, and D2-TFQ systems. These systems were well-stirred for ~3 min at room temperature and left overnight. Third, the generated colored precipitates were removed from the beakers using filter paper, washed three times with the solvent, and oven-dried. Finally, the solid CT complexes were scanned from 400 to 4000 cm^{-1} using an ALPHA Bruker Fourier-Transform Infrared Spectrometer from Bruker Optik GmbH, Germany. The vibrational features of each complex were obtained by comparing the IR spectra of the solid products with those of the corresponding free components (D1, D2, TCNQ, and TFQ).

2.2.3. Elemental analysis

A PerkinElmer Microanalyzer (model 2400 Series II CHNS; USA) determined the carbon, hydrogen, and nitrogen contents (%) for the D1-TCNQ, D2-TCNQ, D1-TFQ, and D2-TFQ solid CT complexes. The elemental composition results were used to verify the molar ratio of the CT reaction between D1 and D2 with the investigated acceptors (TCNQ and TFQ).

2.3. Stoichiometric of the CT reaction in solution state

The stoichiometric of the CT reaction between D1 and D2 with the investigated accepting-molecules (TCNQ and TFQ) in the solution state was obtained using two well-known methods: the spectrophotometric titration method and Job's continuous variation method.

3. Results and discussion

3.1. UV/Visible absorption properties

3.1.1. Free reactants

We found that D1 and D2 donor molecules need slight heat to be dissolved in MeCN, CH_2Cl_2, and $CHCl_3$ solvents, but in MeOH and EtOH solvents, they completely dissolved without any heat. D1 and D2′s solutions in all solvents were colorless. In contrast, the TFQ acceptor is completely soluble in all solvents without any heat, whereas the TCNQ acceptor is easily dissolved in MeCN

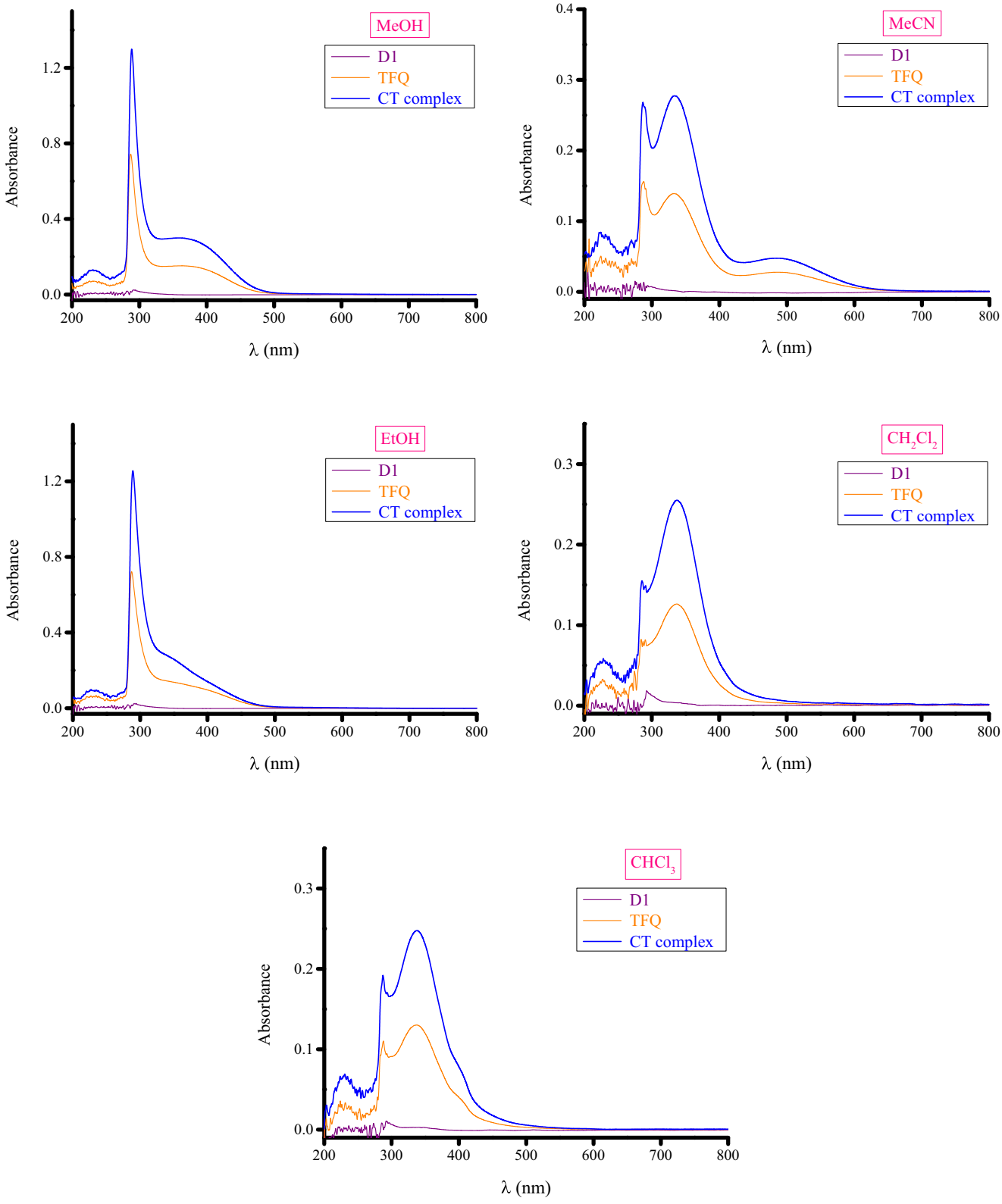

Fig. 9. The UV/Vis spectra of the D1–TFQ complex in MeOH, EtOH, MeCN, CH_2Cl_2, and $CHCl_3$ solvents alongside with their free reactants.

solvent and needs gentle heat to be soluble in the MeOH CH_2Cl_2 and $CHCl_3$ solvents, but it is not soluble in EtOH solvent. Figs. 3 and 4 present the colors of the TCNQ and TFQ solution in the investigated solvents (1.0×10^{-3} M), respectively. Both figures indicate that all the TCNQ and TFQ solutions were colored, and the color varied according to the solvent. The electronic spectra of TCNQ and TFQ acceptors in each solvent (MeOH, EtOH, MeCN, CH_2Cl_2, and $CHCl_3$) are shown in Figs. 5 and 6, respectively.

The TCNQ electronic absorption properties can be classified into two groups:

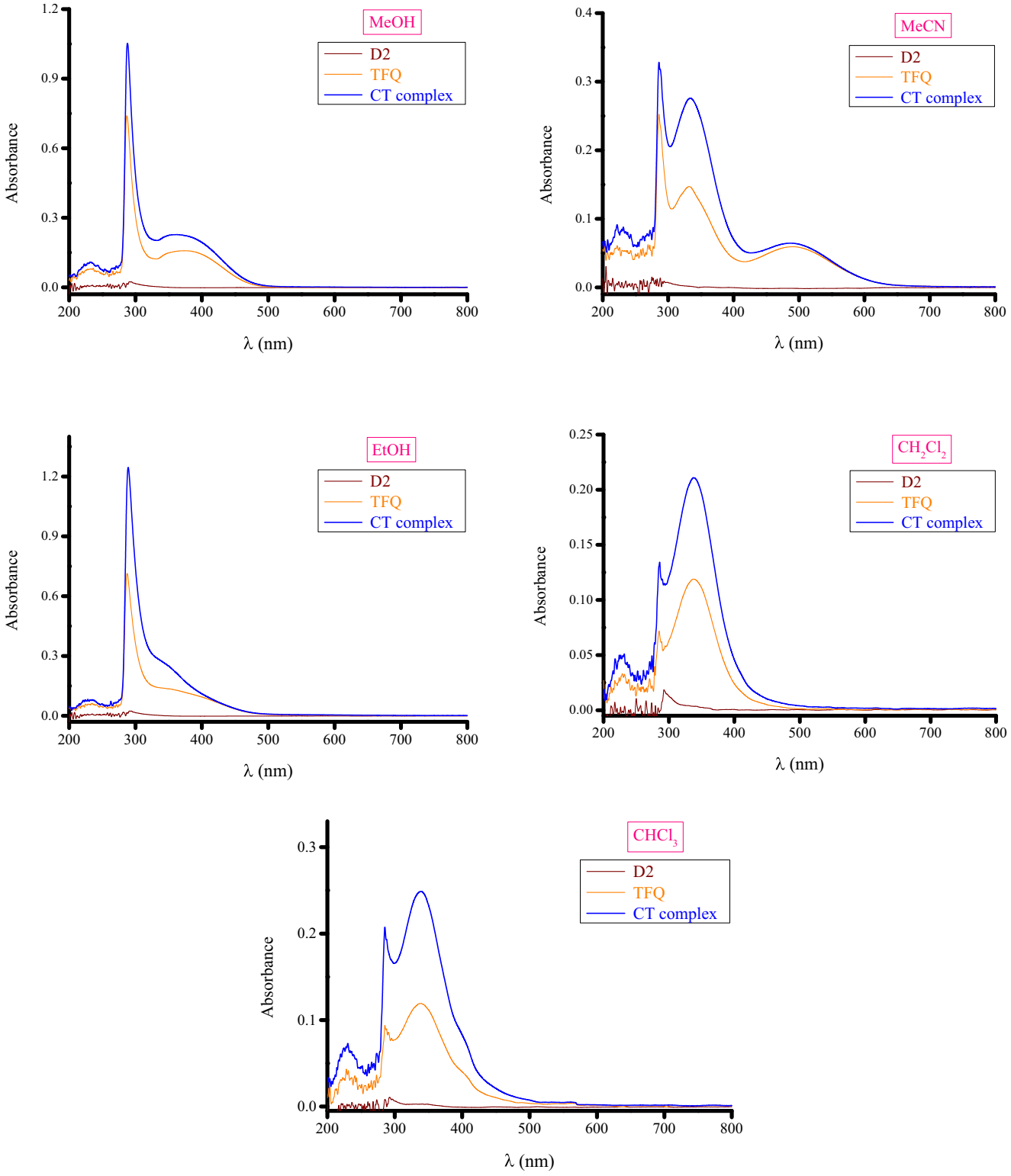

Fig. 10. The UV/Vis spectra of the D2–TFQ complex in MeOH, EtOH, MeCN, CH_2Cl_2, and $CHCl_3$ solvents alongside with their free reactants.

(a) TCNQ in the MeOH solvent:

The TCNQ acceptor creates a light green solution in MeOH solvent. TCNQ in MeOH solvent behaves differently from the other solvents (MeCN, CH_2Cl_2 and $CHCl_3$). The shape and intensity of the UV/Visible spectrum of the TCNQ in MeOH are different from those in the other solvents. Methanolic solution of TCNQ exhibits two intense broad bands that look like a plateau. These two bands centered at 339 and 394 nm. The band's intensity at 339 nm is higher than that at 394 nm. There is also a small broad absorption band found around 740 nm exists in the spectrum of the TCNQ in MeOH.

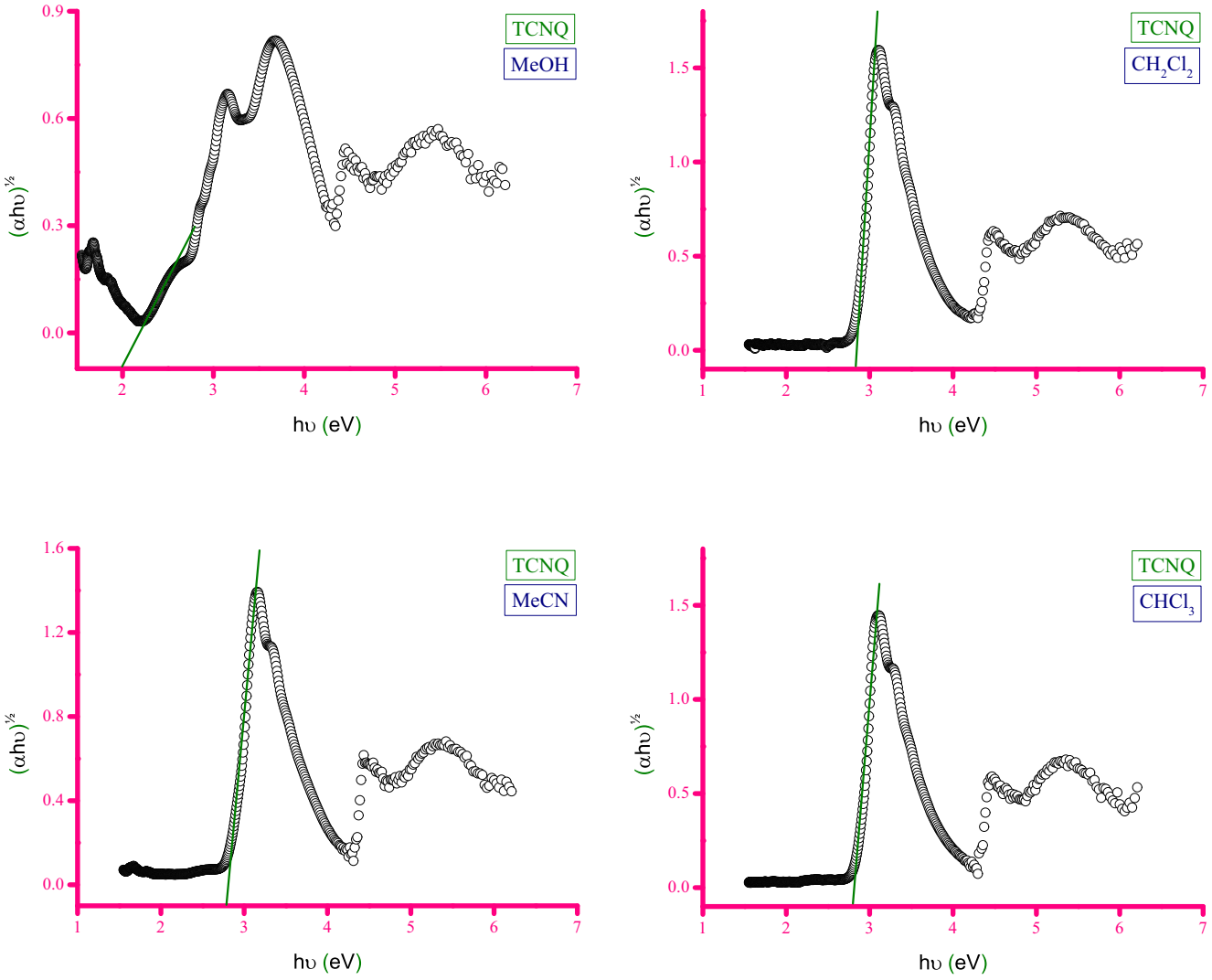

Fig. 11. Tauc's Plots for the TCNQ acceptor dissolved in the investigated solvents.

(b) TCNQ in the MeCN, CH_2Cl_2 and $CHCl_3$ solvents:

TCNQ solution in the MeCN, CH_2Cl_2, and $CHCl_3$ solvents displayed a single, strong, and intense absorption band. This brand has a small shoulder band in all solvents. The width of the band is approximately the same in all solvents, around ~60 nm in width. The maximum of the band (λ^{max}) is 394 nm in MeCN solvent and 400 nm in CH_2Cl_2 and $CHCl_3$ solvents.

Also, the TFQ electronic absorption properties can be classified into three groups:

(a) TFQ in the MeOH and EtOH solvents:

TFQ acceptor creates a beige solution in MeOH and EtOH solvents. TFQ behaved similarly in these two solvents. It created two absorption bands. A sharp and very strong band appeared at 287 nm in both solvents, and this sharp band was coupled with a less intense broadband ranging from 330 to 485 nm. The shape of the broadband is slightly different; in MeOH solvent, it looks like a dome (λ^{max} = 362 nm), but in EtOH solvent, it looks like a plateau (λ^{max} = 340 nm).

(b) TFQ in the MeCN solvent:

The TFQ acceptor forms a remarkable solution in MeCN solvent compared with its solution in other solvents. The color of TFQ's solution in MeOH, EtOH, CH_2Cl_2, and $CHCl_3$ solvents ranged from beige to light-yellow, but in MeCN solvent, TFQ gives a distinguish light-pink color. TFQ's solution in MeOH, EtOH, CH_2Cl_2, and $CHCl_3$ solvents absorbs until 485 nm, but in its acetonitrile solution, its absorption extended to 600 nm. Two absorption bands appeared in the spectrum of TFQ's solution in MeCN solvent. These bands were accumulated at 332 and 487 nm. Both bands were broad, but the band's intensity at 332 nm is 5-times that at 487 nm. The band at 332 nm was coupled with a small shoulder band at 287 nm. This shoulder appears as a very strong and sharp band in the spectrum of TFQ's solution in MeOH and EtOH solvents.

(c) TFQ in the CH_2Cl_2 and $CHCl_3$ solvents:

A single board absorption band was found in the UV/Visible spectra of TFQ's solutions in CH_2Cl_2 and $CHCl_3$ solvents. This broad-

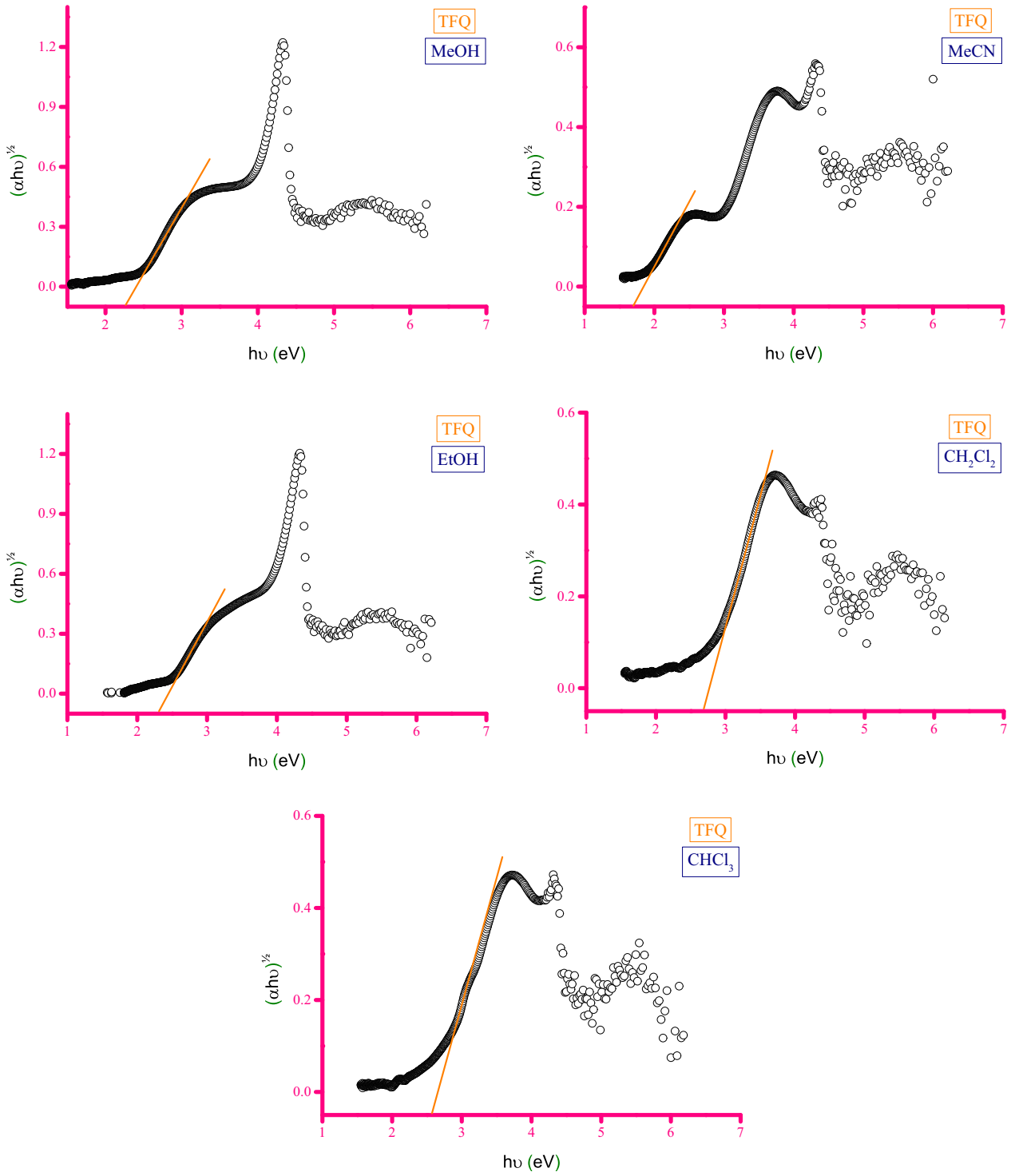

Fig. 12. Tauc's Plots for the TFQ acceptor dissolved in the investigated solvents.

Table 2
Values of E_g derived from Tauc's plots for acceptors alone and their CT complexes with D1 and D2.

Compound	E_g (eV)				
	MeOH	EtOH	MeCN	CH_2Cl_2	$CHCl_3$
TCNQ acceptor	1.99	–	2.79	2.83	2.80
TFQ acceptor	2.28	2.32	1.72	2.69	2.58
D1–TCNQ complex	2.08	–	2.86	2.85	2.81
D2–TCNQ complex	1.86	–	2.75	2.81	2.77
D1–TFQ complex	2.18	2.00	1.40	2.55	2.31
D2–TFQ complex	2.26	2.19	1.65	2.63	2.32

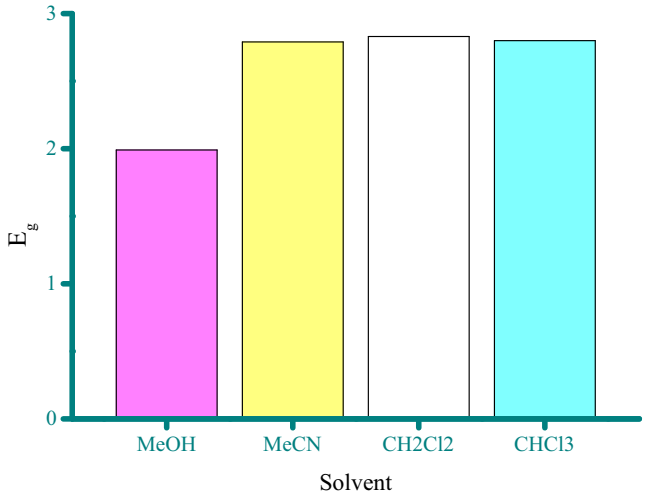

Fig. 13. Comparison of E_g values for TCNQ solutions in the investigated solvents.

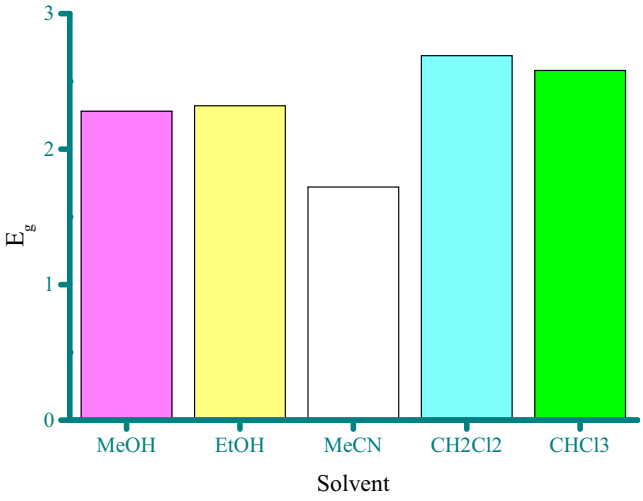

Fig. 14. Comparison of E_g values for TFQ solutions in the investigated solvents.

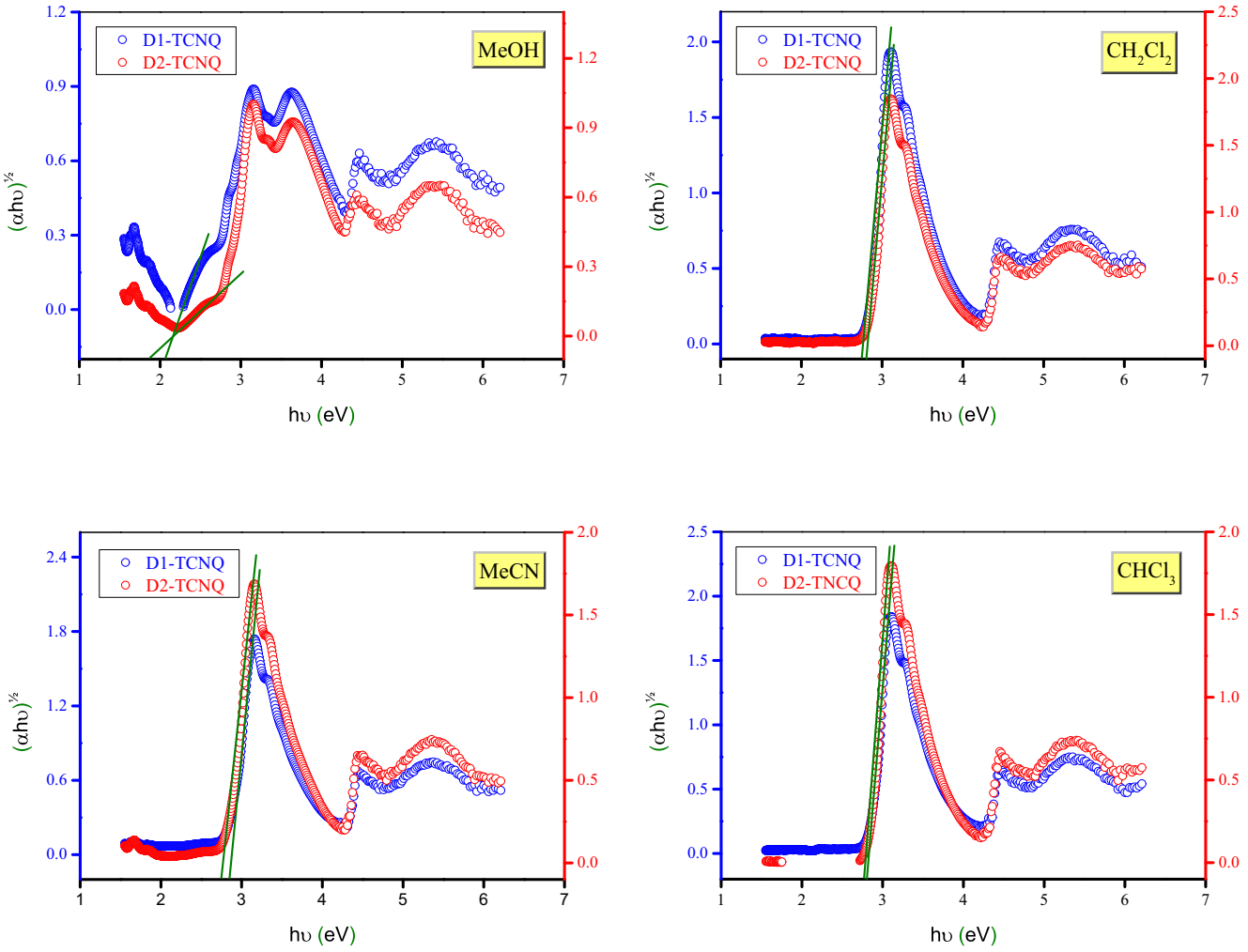

Fig. 15. Tauc's Plots for the D1-TCNQ and D2-TCNQ complexes prepared in the investigated solvents.

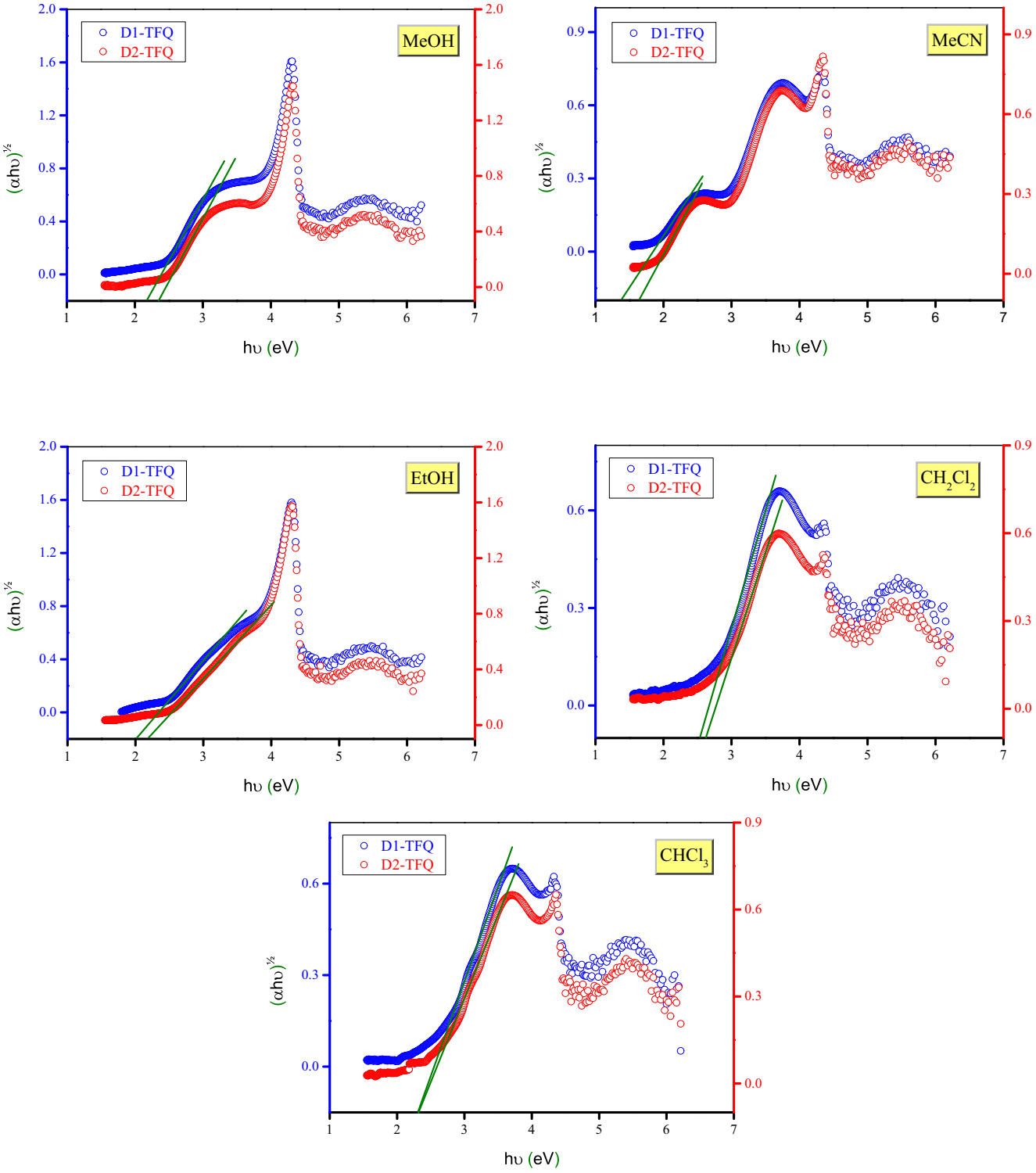

Fig. 16. Tauc's Plots for the D1-TFQ and D2-TFQ complexes prepared in the investigated solvents.

Table 3
Carbon, nitrogen, and hydrogen contents (in %) for the D1 and D2 complexes prepared in different solvents.

Solvent	D1–TCNQ complex						D2–TCNQ complex					
	Carbon		Hydrogen		Nitrogen		Carbon		Hydrogen		Nitrogen	
	Obtained	Calc.	Obtained	Calc.	Obtained	Calc.	Obtained	Calc.	Obtained	Calc.	Obtained	Calc.
MeOH	69.65	69.88	6.15	6.00	9.67	9.88	68.21	68.40	5.40	5.53	9.60	9.39
MeCN	69.66	69.88	6.12	6.00	10.00	9.88	68.65	68.40	5.50	5.53	9.45	9.39
CH_2Cl_2	70.06	69.88	6.18	6.00	10.02	9.88	68.62	68.40	5.48	5.53	9.37	9.39
$CHCl_3$	70.05	69.88	5.80	6.00	9.70	9.88	68.27	68.40	5.55	5.53	9.52	9.39
	D1–TFQ complex						D2–TFQ complex					
	Carbon		Hydrogen		Nitrogen		Carbon		Hydrogen		Nitrogen	
	Obtained	Calc.	Obtained	Calc.	Obtained	Calc.	Obtained	Calc.	Obtained	Calc.	Obtained	Calc.
MeOH	59.48	59.72	5.70	5.53	–	–	58.84	58.69	5.00	5.06	–	–
EtOH	59.70	59.72	5.68	5.53	–	–	58.80	58.69	5.13	5.06	–	–
MeCN	59.55	59.72	5.55	5.53	–	–	58.63	58.69	5.03	5.06	–	–
CH_2Cl_2	59.77	59.72	5.52	5.53	–	–	58.62	58.69	4.96	5.06	–	–
$CHCl_3$	59.61	59.72	5.43	5.53	–	–	58.47	58.69	5.29	5.06	–	–

band is in the range of 280–420 nm, and it has a weak shoulder band at 287 nm. The intensities of the characteristic's absorption bands of TFQ's solutions in different solvents decreased as follow: MeOH > EtOH > MeCN > $CHCl_3$ > CH_2Cl_2. Wavelengths (in nm) of the characteristic absorption bands appeared when TCNQ and TFQ were dissolved in MeOH, EtOH, MeCN, $CHCl_3$, and CH_2Cl_2 solvents (Table 1).

3.1.2. CT complexes

Figs. 7 and 8 contain the UV/Vis spectra of the D1–TCNQ and D2–TCNQ complexes in the MeOH, MeCN, CH_2Cl_2, and $CHCl_3$ solvents alongside that of the free reactants, respectively. The corresponding spectra of the D1–TFQ and D2–TFQ complexes are presented in Figs. 9 and 10, respectively. Generally, D1 and D2 molecules have similar chemical structures. The main difference between the two molecules is that the D2 molecule possesses a C—F bond, whereas the D1 molecule does not. This structure similarity reflects the similarity of the chemical behavior of D1 and D2 molecules when complexed with TCNQ and TFQ acceptors in all solvents. In general, the generation of a CT complex is characterized by a pronounced change in the solution color during the mixing of the donor and the acceptor solutions in an appropriate solvent. This change in solution color is coupled with the change in the electronic spectra of the free donor or/and free acceptor. The spectral changes could be either a new absorption band that did not exist in the electronic spectrum of free donor and free acceptor, an increase in the intensity of the characteristic band referred to the donor or the acceptor, or both. Analysis of the UV/Vis spectra of the D1–TCNQ, D2–TCNQ, D1–TFQ, and D2–TFQ complexes presented in Figs. 7–10 revealed that the CT complexation of D1 and D2 with TCNQ acceptor in MeOH, MeCN, CH_2Cl_2, and $CHCl_3$, and the CT complexation of D1 and D2 with TFQ acceptor in MeOH, EtOH, MeCN, CH_2Cl_2, and $CHCl_3$ strongly enhanced the intensity of the characteristic bands of free TCNQ and TFQ acceptors in the specific solvent.

3.2. Bandgap energies

Tauc's plot [123–125] was used to determine the minimum energy for an electron to jump from a valence band to a conduction band; bandgap energy (termed as E_g). Figs. 11 and 12 contain the Tauc's plots for the TCNQ and TFQ acceptors dissolved in the investigated solvents, respectively. The derived values of E_g are tabulated in Table 2. The E_g value of the TCNQ and TFQ acceptors depends on the solvent's type, as indicated in Figs. 13 and 14. The highest E_g value was displayed by TCNQ solution dissolved in CH_2Cl_2 solvent, where the methanolic solution of TCNQ had the lowest value of E_g. Interestingly, the TFQ acceptor shows the same outcome. Its solution in CH_2Cl_2 solvent had the highest E_g value, whereas its solution in MeOH solvent had the lowest E_g value. Tauc's Plots for the D1-TCNQ and D2-TCNQ complexes prepared in the investigated solvents are presented in Fig. 15; those for the D1-TFQ and D2-TFQ complexes are shown in Fig. 16. The derived E_g values for D1-TCNQ, D2-TCNQ, D1-TFQ, and D2-TFQ complexes are tabulated in Table 2. The complexation of TCNQ acceptor with D1 slightly increased the value of E_g in all solvents, but when TCNQ was complexed with D2, the value of E_g was slightly decreased in all solvents. In contrast, the complexation of TFQ acceptor with both D1 and D2 slightly decreased the value of E_g in all solvents.

3.3. Stoichiometric of the CT interactions

The stoichiometric CT reactions between D1 and D2 with the investigated accepting-molecules (TCNQ and TFQ) in the solid-state were verified by the elemental analyses and spectrophotometric titration and Job's continuous analysis variation methods in the solution state. The elemental results (C%, N%, and H%) for the D1–TCNQ, D2–TCNQ, D1–TFQ, and D2–TFQ solid CT complexes collected by a PerkinElmer Microanalyzer are listed in Table 3. The collected elemental results proposed that the CT interactions between D1 with TCNQ and TFQ and D1 with TCNQ and TFQ proceed at a 1:1 M ratio in all investigated solvents. The spectrophotometric titration method and Job's continuous variation method are the most common techniques used to verify the stoichiometry of a chemical reaction in solution stat using UV/Vis absorption spectra. Figs. 17 and 18 represent the composition of D1 and D2 with TCNQ and TFQ acceptors in the investigated solvents obtained by the spectrophotometric titration method, respectively. Figs. 19 and 20 represent the composition of D1 and D2 with TCNQ and TFQ acceptors in the investigated solvents obtained by Job's continuous variation method, respectively. All plots in Figs. 17–20 suggest that the CT interactions between D1 with TCNQ and TFQ and between D1 with TCNQ and TFQ in solution-state proceeds with a

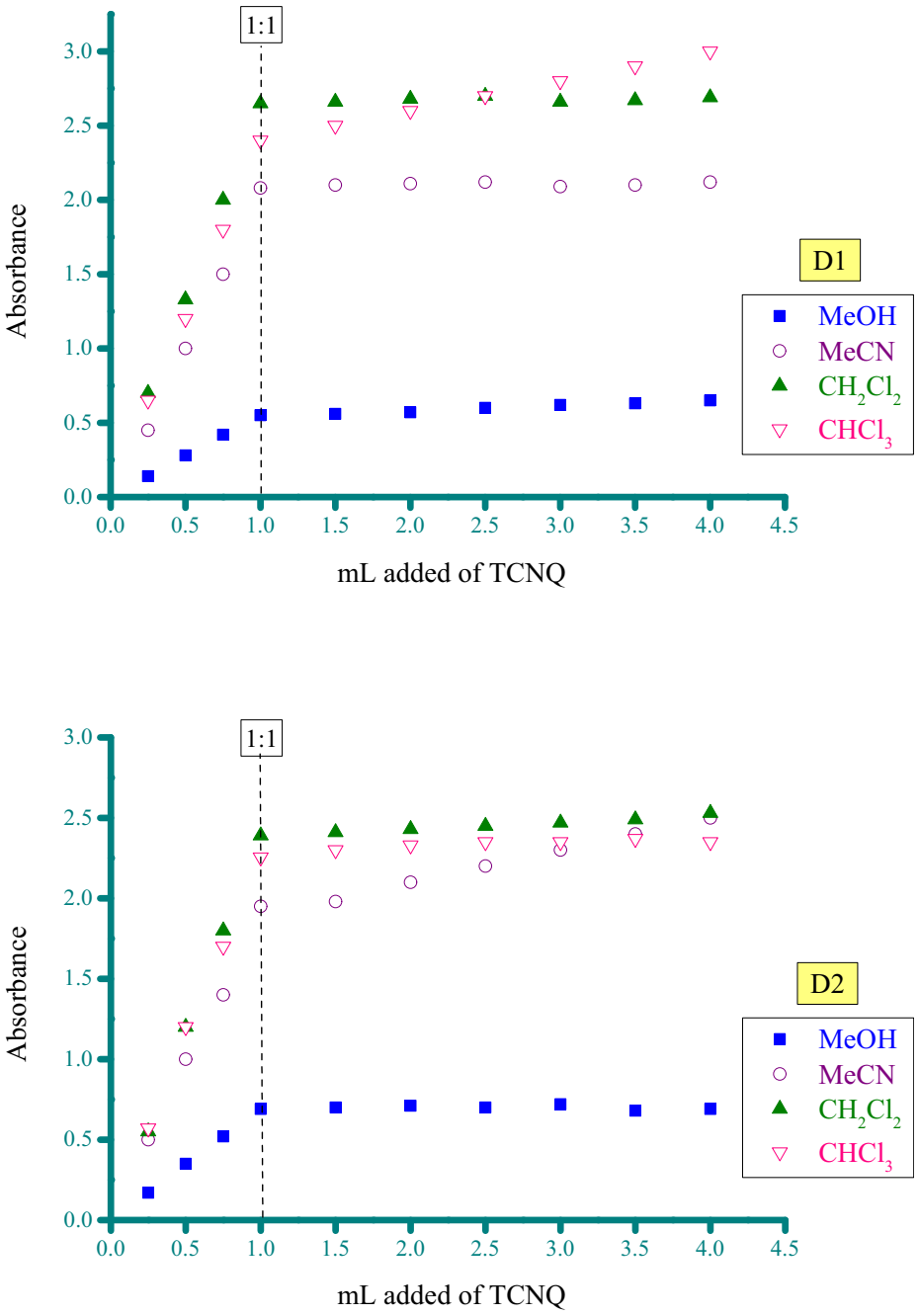

Fig. 17. The composition of D1 and D2 with TCNQ acceptor in the investigated solvents (MeOH, MeCN, CH_2Cl_2, and $CHCl_3$) determined by the spectrophotometric titration method.

molar ratio of 1:1 in all solvents, as observed in the solid-state interaction between the pair components (D1 and TCNQ; D2 and TCNQ; D1 and TFQ; D2 and TFQ).

3.4. Determining spectroscopic parameters

Four common spectroscopic parameters were determined. These parameters were the molar absorptivity (ε_{max}), formation constant (K_{CT}), transition dipole moment (μ_{eg}), and oscillator strength (f) [126–128]. The units of ε_{max}, K_{CT}, and μ_{eg} parameters are (L mol^{-1} cm^{-1}), (L mol^{-1}), and (Debye), respectively. The ε_{max}, K_{CT}, μ_{eg}, and f parameters were calculated for the D1–TCNQ, D2–TCNQ, D1–TFQ, and D2–TFQ complexes in the investigated solvents to understand the CT characteristics from D1 and D2 molecules towards TCNQ and TFQ molecules. Graphical representation of the 1:1 Benesi-Hildebrand equation for the D1 and D2 interactions with TCNQ and TFQ in various solvents are presented in Figs. 21 and 22, respectively. Table 4 lists the derived values of the spectroscopic parameters (K_{CT}, ε_{max}, μ_{eg}, and f) for the D1–TCNQ, D2–TCNQ, D1–TFQ, and D2–TFQ complexes. All the synthesized complexes had high values of K_{CT}. The K_{CT} values for the complexes lie in the range from 1.8×10^6 to 8.8×10^6 L mol^{-1}. D1 and D2 complexes with TCNQ acceptor had very high values of μ_{eg}, and f parameters compared with their complexes with TFQ acceptor.

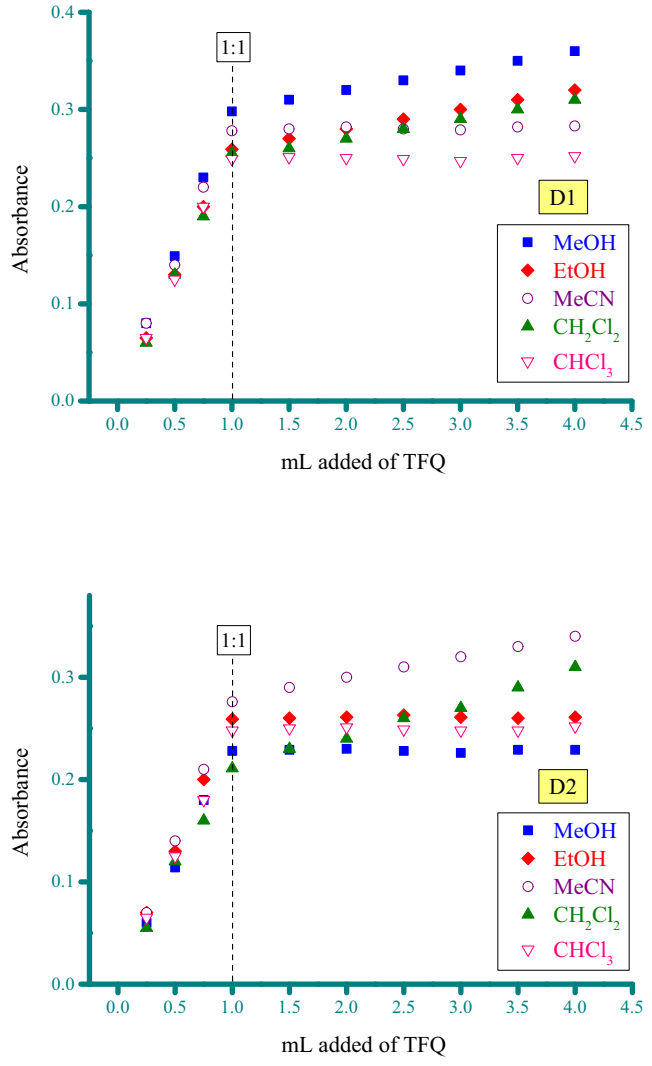

Fig. 18. The composition of D1 and D2 with TFQ acceptor in the investigated solvents (MeOH, EtOH, MeCN, CH_2Cl_2, and $CHCl_3$) obtained by the spectrophotometric titration method.

This outcome suggests a strong interaction between D1 and D2 molecules with TCNQ acceptors with relatively high probabilities for CT transitions [38,69,76,88,102,111,122]. A strong, positive linear correlation between μ_{eg} and f values with Pearson's correlation coefficients (r) lies in the range + 0.9968 – +0.9992 as depicted in Fig. 23. This high mutual relationship between the two parameters (μ_{eg} and f) indicates that the values of μ_{eg} increased as the values of f increased.

3.5. Infrared analysis

Infrared (IR) spectra of pure reactants (D1, D2, TCNQ, and TFQ) are shown in Fig. 24. The intense bands of un-complexed D1 molecule were located at 502 cm^{-1} τ(C—C—C), 566 $\delta_{twi}(CH_2)$, 636 $\delta_{twi}(-CH_3)$, 779 cm^{-1} $\delta_{wag}(CH_2)$, 891 cm^{-1} [$\delta_{wag}(CH_3)$, δ(C—H) deformation], 936 cm^{-1} [δ(O—H) in-plane bending, τ(C—C—O—H)], 1041 cm^{-1} (C—O), 1106 cm^{-1} ν(C—C), 1234 cm^{-1} τ(–CH–C–), 1277 cm^{-1} $\delta_{rock}(CH_2)$, 1351 cm^{-1} $\delta_{sci}(CH_2)$, 1372 cm^{-1} $\delta_{rock}(CH_3)$, 1434 cm^{-1} $\delta_{sci}(CH_3)$, and 1642 cm^{-1} ν(C═O) carbonyl group; 1704 cm^{-1} ν(C═O) carboxylic group; 2920 cm^{-1} [$\nu(CH_3)$, $\nu(CH_2)$], and 3414 cm^{-1} ν(O—H) [Symbol identification: δ_{twi}; twisting, δ_{rock}; rocking, δ_{wag}; wagging, δ_{sci}; scissoring, τ; torsion, δ; bending, ν; stretching]. Un-complexed D2 molecule absorbs at 482 cm^{-1} τ(C—C—C), 536 $\delta_{twi}(CH_2)$, 612 $\delta_{twi}(CH_3)$, 690 cm^{-1} [δ(O—H) out-of-plane bending, ν(C—C)], 761 cm^{-1} $\delta_{wag}(CH_2)$, 855 cm^{-1} τ(C—C—C—H), 897 cm^{-1} [$\delta_{wag}(CH_3)$, δ(C—H) deformation], 984 cm^{-1} [δ(O—H) in-plane bending, τ(C—C—O—H)], 1054 cm^{-1} (C—O), 1127 cm^{-1} ν(C—C), 1207 cm^{-1} τ(—CH—C—), 1239 cm^{-1} $\delta_{rock}(CH_2)$, 1280 cm^{-1} ν(C—F), 1358 cm^{-1} $\delta_{sci}(CH_2)$, 1403 cm^{-1} $\delta_{rock}(CH_3)$, 1448 cm^{-1} $\delta_{sci}(CH_3)$, 1543 ν(C═C), 1660 and 1618 cm^{-1} ν(C═O) carbonyl group; 1713 cm^{-1} ν(C═O) carboxylic group; 2946 cm^{-1} [$\nu(CH_3)$, $\nu(CH_2)$], and 3393 cm^{-1} ν(O—H).

The very strong band observed at 1054 cm^{-1} (D2) and 1041 cm^{-1} (D1) originated from the stretching vibration of the C—O bond. The very strong band observed at 1660 cm^{-1} (D2) and 1642 cm^{-1} (D1) was originated from the stretching vibration of the C═O bond of the carbonyl group, whereas those appeared at 1713 cm^{-1} (D2) and 1704 cm^{-1} (D1) conjugated to the C═O bond of the carboxylic group. The band resonated at 1280 cm^{-1} in the IR spectrum of the D2 could be assigned to the ν(C—F) vibrations [129]. Methyl (CH_3) and methylene (CH_2) groups in D1 and D2 molecules displayed several absorption bands. D1 and D2 molecules possess multiple CH_2 and CH_3 groups [eight CH_2 groups and two CH_3 groups in D1; five CH_2 groups and three CH_3 groups in D2], and these groups make the IR spectrum of D1 and D2 noise complicated, especially in the area from 700 to 1500 cm^{-1}. The bending vibrations of–CH_2 groups: $\delta_{twi}(CH_2)$, $\delta_{wag}(CH_2)$, $\delta_{rock}(CH_2)$, and $\delta_{sci}(CH_2)$ are responsible for the bands located at 566, 779, 1277, and 1351 cm^{-1} in the IR spectrum of D1, respectively. The corresponding wavenumbers for the D2 were 536, 761, 1239, and 1358 cm^{-1}, respectively [130,131]. The bending vibrations of —CH_3 groups: $\delta_{twi}(CH_3)$, $\delta_{wag}(CH_3)$, $\delta_{rock}(CH_3)$, and $\delta_{sci}(CH_3)$ are responsible for the bands located at 636, 890, 1372, and 1434 cm^{-1} in the IR spectrum of D1, respectively. The corresponding wavenumbers for the D2 were 612, 897, 1403, and 1448 cm^{-1}, respectively. The $\nu(CH_2)$ and $\nu(CH_3)$ vibrations create a broad absorption band with a medium-intensity accumulation at 2946 cm^{-1} (D2) and 2920 cm^{-1} (D1). The in-plane bending, out-of-plane bending, and stretching vibrations generated from the O—H bonds in the D1 molecule created the bands at 685, 936, and 3414 cm^{-1}, respectively. The corresponding wavenumbers for the D2 were 690, 984, and 3393 cm^{-1}, respectively.

In the IR spectrum of pure TCNQ, the band at 2216 cm^{-1}, combined with a small broad shoulder at 2282 cm^{-1}, resulted from the molecule's ν(C≡N) vibrations. The four C—H bonds in the TCNQ are absorbed in 855, 1350, 2968, and 3046 cm^{-1} due to the δ_{rock}(-C—H), δ_{def}(C—H), ν_s(C—H), ν_{as}(C—H) modes, respectively. The bands registered at (1052 and 1118) and 1533 cm^{-1} were generated from the δ(C—C) and ν(C═C) vibrations, respectively. The functional groups in the TFQ molecule are two C═C, two C═O, and four C—F. In the IR spectrum of this molecule, the three types of chemical bonds created three intense and very strong bands, registered respectively at 1320, 1680, and 988 cm^{-1}, caused by the ν(C═C), ν(C═O), ν(C—F).

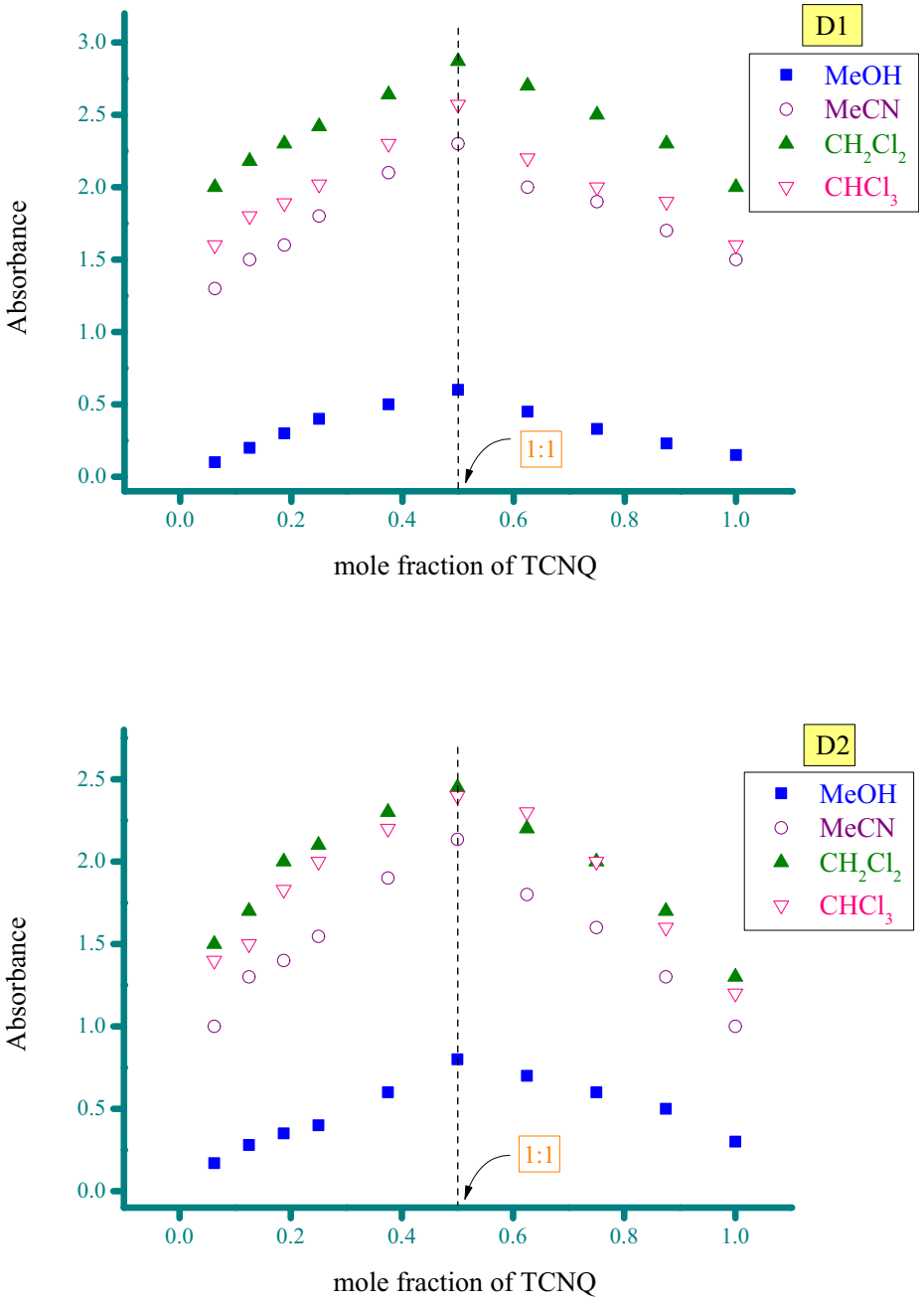

Fig. 19. The composition of D1 and D2 with TCNQ acceptor in the investigated solvents (MeOH, MeCN, CH_2Cl_2, and $CHCl_3$) obtained by the Job's continuous variation method.

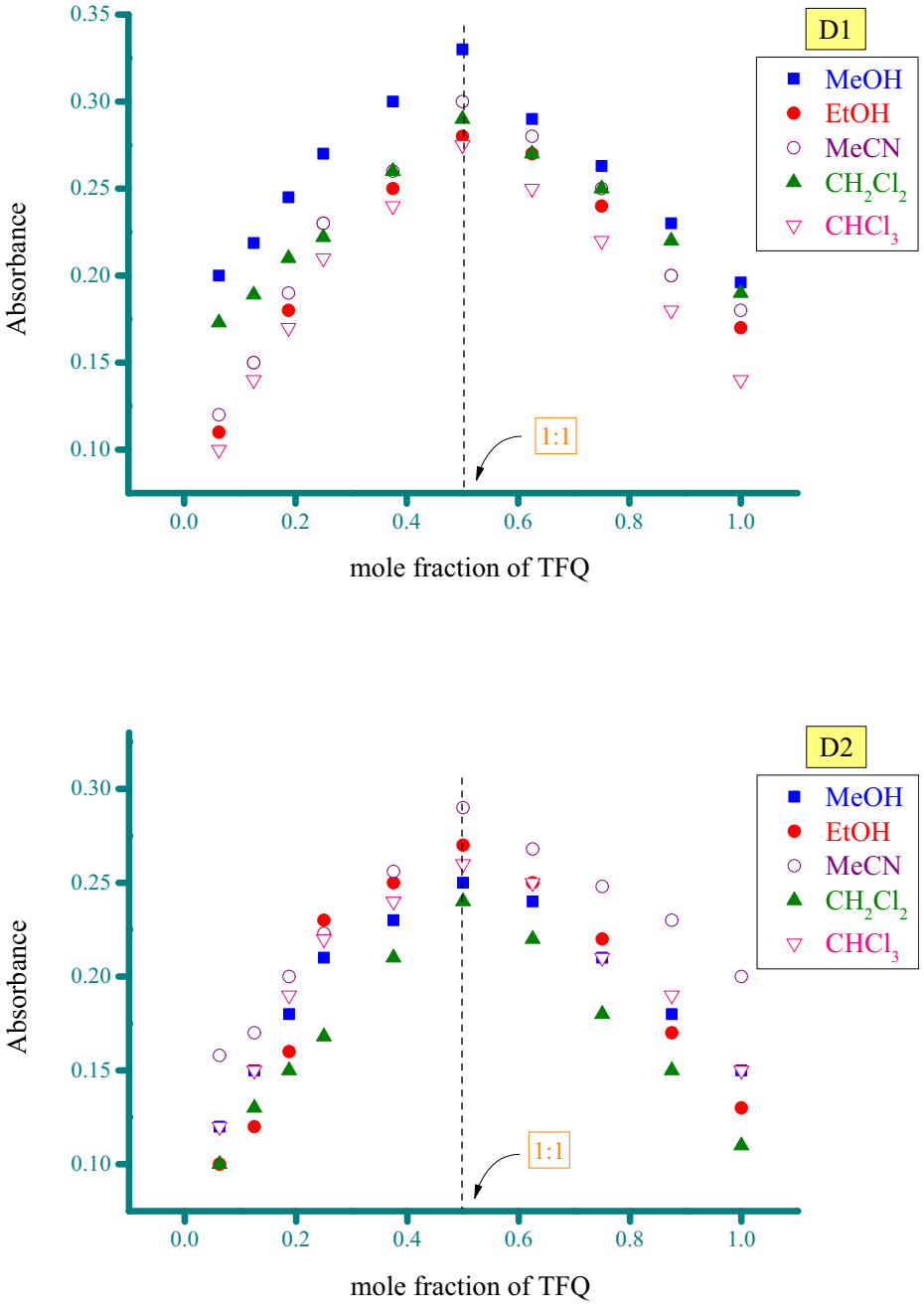

Fig. 20. The composition of D1 and D2 with TFQ acceptor in the investigated solvents (MeOH, MeCN, CH_2Cl_2, and $CHCl_3$) determined by the Job's continuous variation method.

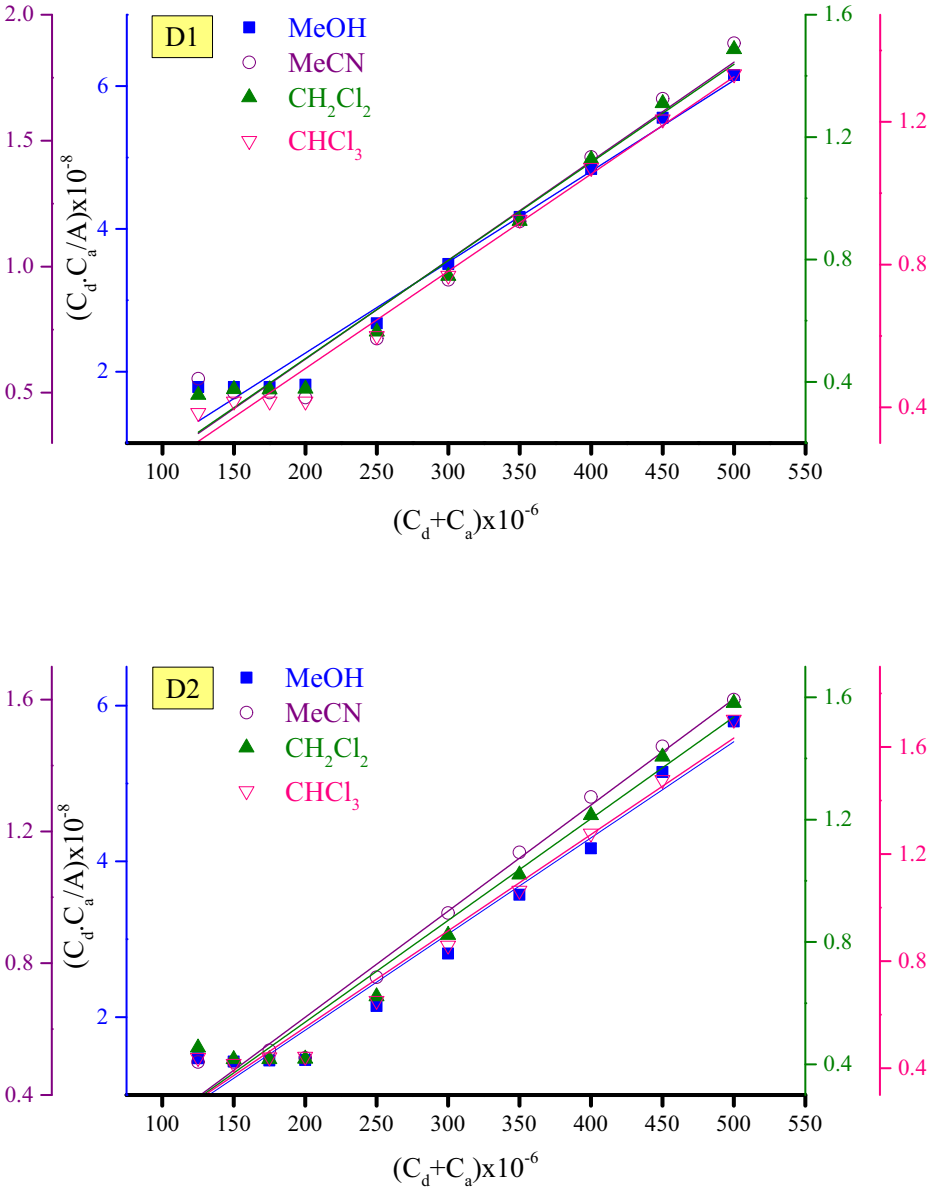

Fig. 21. Graphical representation of the 1:1 Benesi–Hildebrand equation for the D1 and D2 interactions with TCNQ acceptor in the investigated solvents (MeOH, MeCN, CH_2Cl_2, and $CHCl_3$).

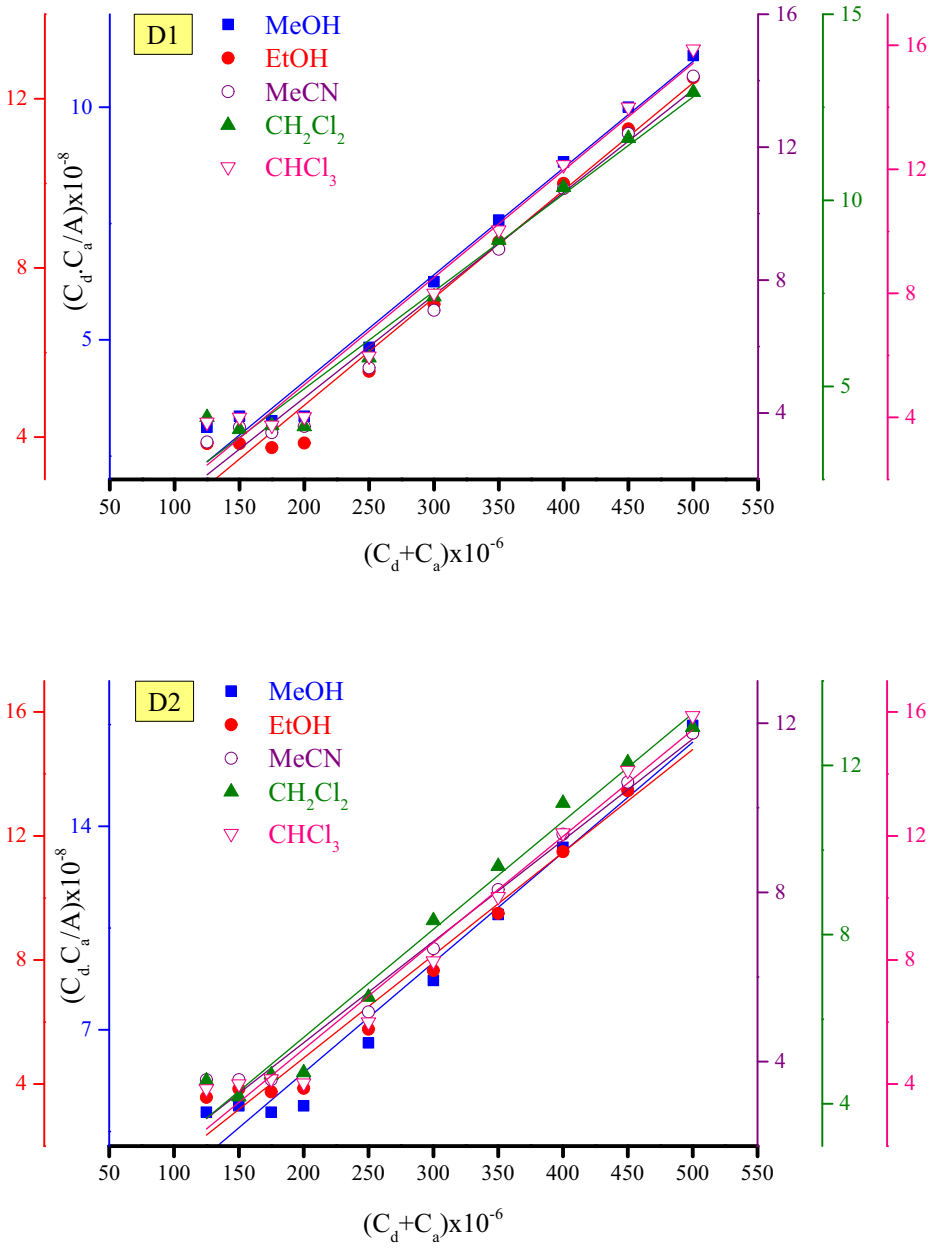

Fig. 22. Graphical representation of the 1:1 Benesi–Hildebrand equation for the D1 and D2 interactions with TFQ acceptor in the investigated solvents (MeOH, EtOH, MeCN, CH_2Cl_2, and $CHCl_3$).

Table 4
The molar absorptivity (ε_{max}), formation constant (K_{CT}), transition dipole moment (μ_{eg}), and oscillator strength (f) for the D1 and D2 complexes prepared in the investigated solvents.

Solvent	D1–TCNQ complex					D2–TCNQ complex				
	λ^{max} (nm)	ε_{max} (L mol^{-1} cm^{-1})	K_{CT} (L mol^{-1})	μ (Debye)	f –	λ^{max} (nm)	ε_{max} (L mol^{-1} cm^{-1})	K_{CT} (L mol^{-1})	μ (Debye)	f –
MeOH	394	7.85×10^5	4.44×10^6	21.7	0.565	394	8.10×10^5	1.94×10^6	22.1	0.582
MeCN	394	2.54×10^6	2.57×10^6	39.2	1.831	394	3.11×10^6	3.96×10^6	43.3	2.235
CH_2Cl_2	400	3.12×10^6	1.94×10^6	43.6	2.242	400	3.01×10^6	2.62×10^6	42.9	2.168
$CHCl_3$	400	3.68×10^6	7.55×10^6	47.4	2.646	400	2.78×10^6	2.15×10^6	41.2	1.999
	D1–TFQ complex					D2–TFQ complex				
	λ^{max} (nm)	ε_{max} (L mol^{-1} cm^{-1})	K_{CT} (L mol^{-1})	μ (Debye)	f –	λ^{max} (nm)	ε_{max} (L mol^{-1} cm^{-1})	K_{CT} (L mol^{-1})	μ (Debye)	f –
MeOH	362	4.36×10^5	4.69×10^6	12.00	0.188	362	2.64×10^5	1.85×10^6	9.37	0.114
EtOH	340	3.93×10^5	7.71×10^6	11.08	0.170	340	3.02×10^5	1.86×10^6	9.70	0.130
MeCN	333	3.24×10^5	1.79×10^6	11.12	0.175	333	4.18×10^5	6.97×10^6	12.63	0.226
CH_2Cl_2	337	3.82×10^5	8.88×10^6	12.16	0.207	337	3.92×10^5	5.48×10^6	12.30	0.212
$CHCl_3$	337	2.89×10^5	1.86×10^6	10.58	0.156	337	2.91×10^5	1.97×10^6	10.60	0.157

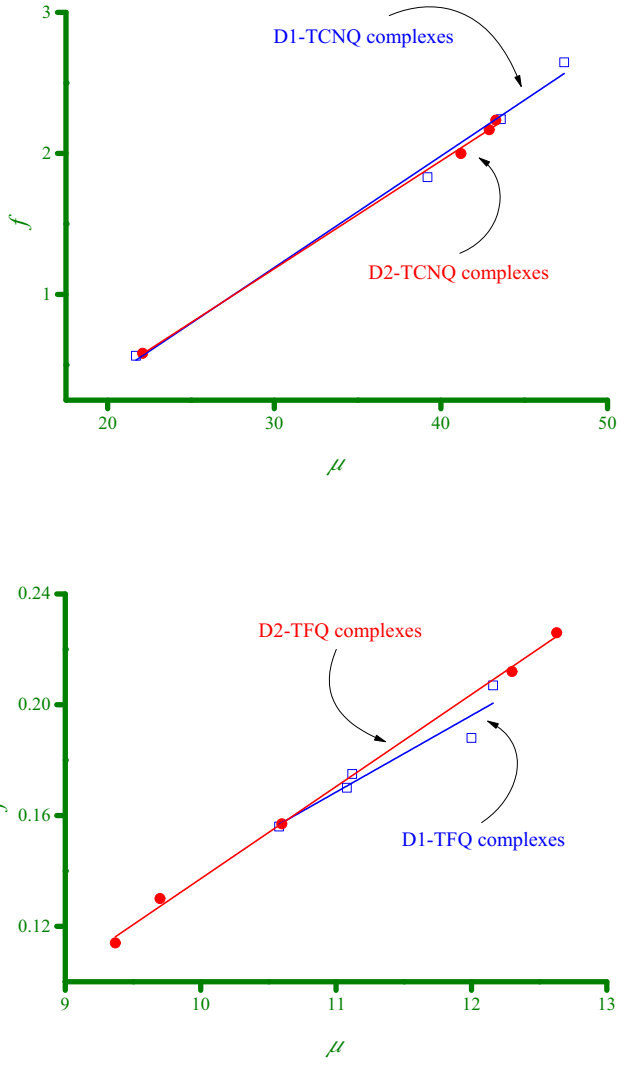

Fig. 23. Linear relationship between oscillator strength (f) and transition dipole moment (μ_{eg}).

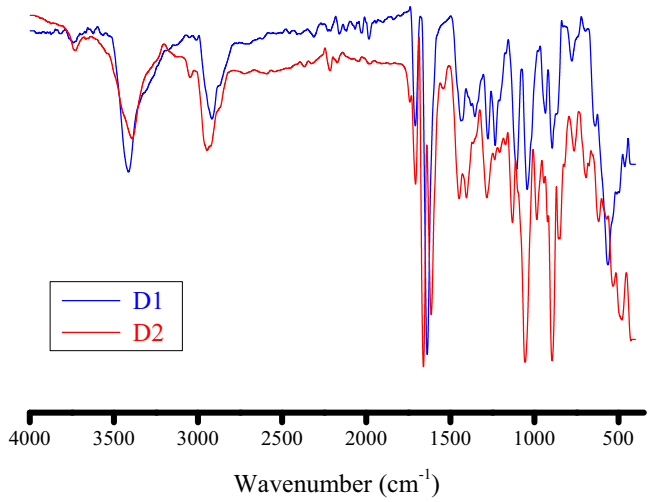

Fig. 24a. IR spectra of free D1 and D2 molecules.

TCNQ and TFQ molecules are typical electron-accepting units because they contain strong terminal electron-withdrawing groups. When a molecule possesses terminal electron-withdrawing groups, they take the electron density from the molecule's core, making the core deficient in electron density and thirsty to accept electronic charges from another molecule (electron-donating molecule). The terminal electron-withdrawing groups in TCNQ are the four C≡N groups and are the two C═O and four C—F groups in TFQ. These withdrawing groups greatly decrease the electron density of the TCNQ and TFQ's aromatic rings and increase the aromatic ring's need for electrons. When mixing solutions of D1 or D2 with solutions of TCNQ or TFQ, electron charges were transferred from the donating sites in the electron-donating molecule (D1 or D2) to the aromatic ring of the electron-accepting molecule (TCNQ or TFQ) [D1 → TCNQ; D2 → TCNQ; D1 → TFQ; D2 → TFQ]. This donating-accepting interaction affects the solution's color, the distinguish electronic spec-

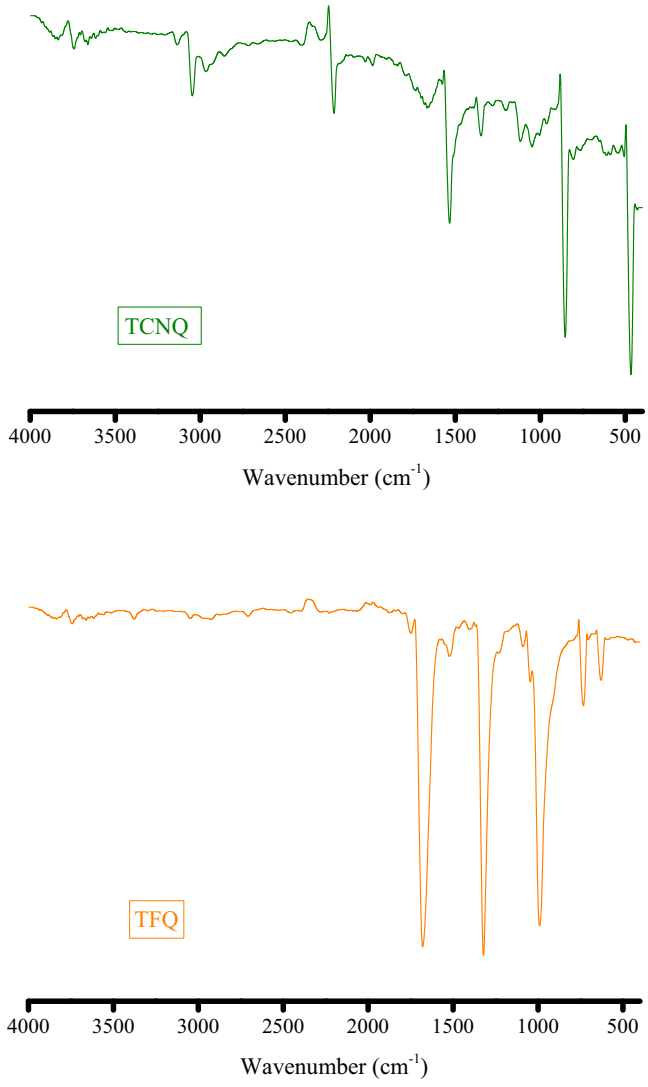

Fig. 24b. IR spectra of free TCNQ and TFQ molecules.

tral bands of the free reactants, and the distinguish IR spectral bands of the free reactants.

The IR spectra displayed in Fig. 25 are for the solid D1–TCNQ, D2–TCNQ, D1–TFQ, and D2–TFQ complexes generated in different solvents. These IR spectra revealed several spectral changes in the distinguish IR bands of free reactants (D1, D2, TCNQ, TFQ) after the CT complexation. Here we mentioned three examples: i) The bands resulting from the C═O stretching vibrations of the carbonyl and carboxylic groups of free D1 and D2 shifted to lower frequencies after CT complexation with TCNQ and TFQ. From 1704–1642 cm^{-1} in the free D1 to around ~1686–1630 cm^{-1} in the D1–TCNQ and D1–TFQ complexes. The same was detected for the D2; the bands were moved from 1713–1660 cm^{-1} to around ~1700–1642 cm^{-1} in the D2–TCNQ and D2–TFQ complexes. ii). The CT complexation between TCNQ with D1 and D2 affected the intensity and position of the characteristic bands belonging to the ν(C≡N) in the free TCNQ. The position of the bands was moved from 2216 and 2282 cm^{-1} in the free TCNQ to around ~2190 and 2210 cm^{-1} in its complexes with D1 and D2 (D1–TCNQ, D2–TCNQ). iii) In the free TFQ, the ν(C—F) vibrations resonated at 988 cm^{-1} as a very strong, intense band, but in the D1–TFQ and D2–TFQ complexes, this was appeared at around ~1020 cm^{-1} as a medium intensity band.

4. Conclusions

Hydrocortisone (D1) and dexamethasone (D2) have received considerable attention because they are widely used to treat COVID-19. We aim to furnish a big-picture perspective on the charge-transfer (CT) properties of corticosteroids D1 and D2. In part I, we examined the CT property of D1 and D2 towards the DDQ accepting-molecule in five different organic solvents. This part (part II) described the CT reaction between D1 and D2 with two new organic accepting-molecules (TCNQ and TFQ) in five different organic solvents. Calculated values of oscillator strength (*f*) and transition dipole moment (μ_{eg}) suggested that the interaction between the investigated corticosteroids with TCNQ acceptor is much stronger than their interaction with TFQ acceptor. IR measurements suggested that electron charges transferred from the donating sites in D1 and D2 to the aromatic ring of TCNQ and TFQ (n → π* transitions).

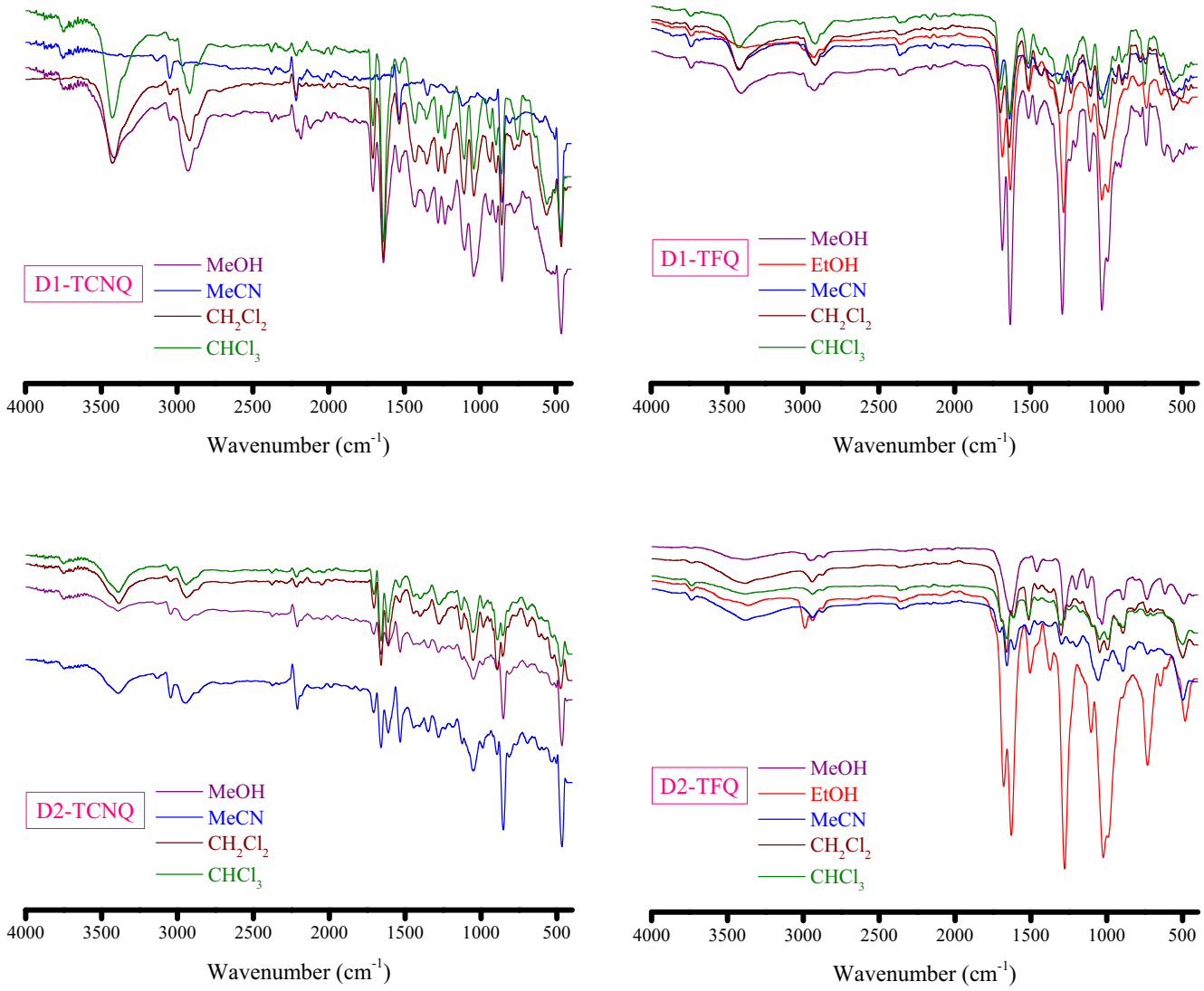

Fig. 25. IR spectra of the D1–TCNQ, D2–TCNQ, D1–TFQ, and D2–TFQ complexes prepared in various solvents.

CRediT authorship contribution statement

Moamen S. Refat: Data curation, Funding acquisition, Project administration, Writing – original draft, Writing – review & editing. **Bander Albogami:** Supervision, Conceptualization, Software, Validation, Visualization. **Abdel Majid A. Adam:** Data curation, Funding acquisition, Project administration, Writing – original draft, Writing – review & editing. **Hosam A. Saad:** Investigation, Formal analysis, Methodology, Resources. **Amnah Mohammed Alsuhaibani:** Investigation, Formal analysis, Methodology, Resources. **Lal Miyan:** Supervision, Conceptualization, Software, Validation, Visualization. **Mohamed S. Hegab:** Investigation, Formal analysis, Methodology, Resources.

Data availability

Data will be made available on request.

Declaration of Competing Interest

The authors declare that they have no known competing financial interests or personal relationships that could have appeared to influence the work reported in this paper.

Acknowledgments

This work was supported by Taif University Researchers Supporting Project Number (TURSP-2020/02), Taif University, Taif, Saudi Arabia.

References

[1] J. Andreani, M. Le Bideau, I. Duflot, P. Jardot, C. Rolland, M. Boxberger, N. Wurtz, J. Rolain, P. Colson, B. La Scola, D. Raoult, *In vitro* testing of combined hydroxychloroquine and azithromycin on SARS-CoV-2 shows synergistic effect, Microb. Pathog. 145 (2020) 104228.
[2] N. Zhu, D. Zhang, W. Wang, X. Li, B. Yang, J. Song, X. Zhao, B. Huang, W. Shi, R. Lu, P. Niu, F. Zhan, X. Ma, D. Wang, W. Xu, G. Wu, G.F. Gao, D. Phil. W. Tan, A novel coronavirus from patients with pneumonia in China, 2019, N. Engl. J. Med. 382 (2020) 727-733.
[3] Organization WH, WHO director-General's opening remarks at the media briefing on COVID-19, 11 March 2020, Geneva, Switzerland, 2020.
[4] L. Pasin, P. Navalesi, A. Zangrillo, A. Kuzovlev, V. Likhvantsev, L.A. Hajjar, S. Fresilli, M.V.G. Lacerda, G. Landoni, Corticosteroids for Patients With Coronavirus Disease 2019 (COVID-19) With Different Disease Severity: A Meta-Analysis of Randomized Clinical Trials, J. Cardiothorac. Vasc. Anesth. 35 (2) (2021) 578–584.
[5] Johns Hopkins Coronavirus Resource Center, COVID-19 Data in Motion, Accessed August 30, 2021. https://coronavirus.jhu.edu.
[6] M. Alkotaji, Azithromycin and ambroxol as potential pharmacotherapy for SARS-CoV-2, Int. J. Antimicrob. Agents 56 (6) (2020) 106192.

[7] Y. Zheng, J. Shang, Y. Yang, C. Liu, Y. Wan, Q. Geng, M. Wang, R. Baric, F. Li, Lysosomal proteases are a determinant of coronavirus tropism, J. Virol. 92 (2018) e01504–e01518.

[8] D. Annane, Corticosteroids for COVID-19, J. Intensive Med. 1 (2021) 14–25.

[9] M.A. Gonzalez-Moles, P. Morales, A. Rodriguez-Archilla, I.R. Isabel, S. Gonzalez-Moles, Treatment of severe chronic oral erosive lesions with clobetasol propionate in aqueous solution, Oral Surg. Oral Med. Oral Pathol. Oral Radiol. Endod. 93 (3) (2002) 264–270.

[10] M. Kosaka, Y. Yamazaki, T. Maruno, K. Sakaguchi, S. Sawaki, Corticosteroids as adjunctive therapy in the treatment of coronavirus disease 2019: A report of two cases and literature review, J. Infect. Chemother. 27 (2021) (2019) 94–98.

[11] A.K. Singh, S. Majumdar, R. Singh, A. Misra, Diabetes Metab. Syndr.: Clin. Res. Rev. 14 (2020) 971-978.

[12] S.C. Sweetman (Ed.), Martindale: The Complete Drug Reference, 37th ed., Pharmaceutical Press, London, England, UK, 2011.

[13] E.J. Cano, X.F. Fuentes, C.C. Campioli, J.C. O'Horo, O.A. Saleh, Y. Odeyemi, H. Yadav, Z. Temesgen, Impact of corticosteroids in coronavirus disease 2019 outcomes, Chest 159 (3) (2021) 1019–1040.

[14] R. Huang, C. Zhu, J. Wang, L. Xue, C. Li, X. Yan, S. Huange, B. Zhang, L. Zhu, T. Xu, F. Ming, Y. Zhao, J. Cheng, H. Shao, X. Zhao, D. Sang, H. Zhao, X. Guan, X. Chen, Y. Chen, J. Wei, R. Issa, L. Liu, X. Yan, C. Wu, Corticosteroid therapy is associated with the delay of SARS-CoV-2 clearance in COVID-19 patients, Eur. J. Pharmacol. 889 (2020) 173556.

[15] K. Chatterjee, C. Wu, A. Bhardwaj, M. Siuba, Steroids in COVID-19: An overview, Cleve. Clin. J. Med. 20 (Aug 2020), https://doi.org/10.3949/ccjm.87a.ccc059.

[16] N. Sharma, A.S. Reddy, K. Yun, Chemosphere 282 (2021) 131029.

[17] C. Liu, Z. Zhou, G. Liu, Q. Wang, J. Chen, L. Wang, Y. Zhou, G. Dong, X. Xu, Y. Wang, Y. Guo, M. Lin, L. Wu, G. Du, C. Wei, X. Zeng, X. Wang, J. Wu, H. Zhou, Efficacy and Safety of Dexamethasone Ointment on Recurrent Aphthous Ulceration, Am. J. Med. 125 (3) (2012) 292–301.

[18] K. Allen, Dexamethasone: An all purpose agent?, Australasian Anaesthesia (2007) 65–70

[19] A.E. Coutinho, K.E. Chapman, The anti-inflammatory and immunosuppressive effects of glucocorticoids, recent developments and mechanistic insights, Mol. Cell. Endocrinol. 335 (1) (2011) 2–13.

[20] S. Shakya, I.M. Khan, Charge transfer complexes: Emerging and promising colorimetric real-time chemosensors for hazardous materials, J. Hazard. Mater. 403 (2021) 123537.

[21] A.S. Al-Attas, M.M. Habeeb, D.S. Al-Raimi, Spectrophotometric determination of some amino heterocyclic donors through charge transfer complex formation with chloranilic acid in acetonitrile, J. Mol. Liq. 148 (2–3) (2009) 58–66.

[22] J. Seliger, V. Zagar, K. Gotoh, H. Ishida, A. Konnai, D. Amino, T. Asaji, Hydrogen bonding in 1,2-diazine–chloranilic acid (2:1) studied by a ^{14}N nuclear quadrupole coupling tensor and multi-temperature X-ray diffraction, Phys. Chem. Chem. Phys. 11 (13) (2009) 2281–2286.

[23] A.S. Gaballa, C. Wagner, S.M. Teleb, E.M. Nour, M.A.F. Elmosallamy, G.N. Kaluderovic, H. Schmidt, D. Steinborn, Preparation, spectroscopic and structural studies on charge-transfer complexes of 2,9-dimethyl-1,10-phenanthroline with some electron acceptors, J. Mol. Struct. 876 (1–3) (2008) 301–307.

[24] R.S. Mulliken, W.B. Person, Molecular Complexes, Wiley, New York, 1969.

[25] R.S. Mulliken, Structures of complexes formed by halogen molecules with aromatic and with oxygenated solvents, J. Am. Chem. Soc. 72 (1950) 600–608.

[26] R. Foster, Organic Charge-Transfer Complexes, Academic Press, London, 1969.

[27] R.S. Mulliken, Molecular Compounds and their Spectra. III. The Interaction of Electron Donors and Acceptors, J. Phys. Chem. 56 (7) (1952) 801–822.

[28] Mohd. Akram, Hira Lal, Sonam Shakya, Kabir-ud-Din, Multispectroscopic and Computational Analysis Insight into the Interaction of Cationic Diester-Bonded Gemini Surfactants with Serine Protease α-Chymotrypsin, CS Omega 5 (7) (2020) 3624-3637.

[29] S. Shakya, I.M. Khan, M. Ahmad, Charge transfer complex based real-time colorimetric chemosensor for rapid recognition of dinitrobenzene and discriminative detection of Fe^{2+} ions in aqueous media and human hemoglobin, J. Photochem. Photobiol., A 392 (2020) 112402.

[30] Ashraf El-Bindary, Zeinab Anwar, Taissir El-Shafaie, Effect of silicon dioxide nanoparticles on the assessment of quercetin flavonoid using Rhodamine B Isothiocyanate dye, J. Mol. Liq. 323 (2021) 114607.

[31] A.M.A. Adam, H.A. Saad, A.A. Atta, M. Alsawat, M.S. Hegab, T.A. Altalhi, M.S. Refat, Utilization of charge-transfer complexation to generate carbon-based nanomaterial for the adsorption of pollutants from contaminated water: Reaction between urea and vacant *orbital* acceptors, J. Mol. Liq. 341 (2021) 117416.

[32] M.S. Refat, H.A. Saad, A.A. Gobouri, M. Alsawat, A.M.A. Adam, S.M. El-Megharbel, Charge transfer complexation between some transition metal ions with azo Schiff base donor as a smart precursor for synthesis of nano oxides: An adsorption efficiency for treatment of Congo red dye in wastewater, J. Mol. Liq. (2021), https://doi.org/10.1016/j.molliq.2021.117140 117140.

[33] A.M.A. Adam, M.S. Refat, T.A. Altalhi, F.S. Aldawsari, G.H. Al-Hazmi, Liquid- and solid-stae study of charge-transfer (CT) interaction between drug triamterene as a donor and tetracyanoethylene (TCNE) as an acceptor, J. Mol. Liq. 336 (2021) 116261.

[34] A.M.A. Adam, M.S. Refat, T.A. Altalhi, K.S. Alsuhaibani, Charge-transfer complexation of TCNE with azithromycin, the antibiotic used worldwide to treat the coronavirus disease (COVID-19). Part IV: A comparison between solid and liquid interactions, J. Mol. Liq. 340 (2021) 117224.

[35] A.M.A. Adam, H.A. Saad, A.M. Alsuhaibani, M.S. Refat, M.S. Hegab, Charge-transfer chemistry of azithromycin, the antibiotic used worldwide to treat the coronavirus disease (COVID-19). Part III: A green protocol for facile synthesis of complexes with TCNQ, DDQ, and TFQ acceptors, J. Mol. Liq. 335 (2021) 116250.

[36] A.M.A. Adam, H.A. Saad, A.M. Alsuhaibani, M.S. Refat, M.S. Hegab, Charge-transfer chemistry of azithromycin, the antibiotic used worldwide to treat the coronavirus disease (COVID-19). Part II: Complexation with several π-acceptors (PA, CLA, CHL), J. Mol. Liq. 325 (2021) 115121.

[37] A.M.A. Adam, H.A. Saad, A.M. Alsuhaibani, M.S. Refat, M.S. Hegab, Charge-transfer chemistry of azithromycin, the antibiotic used worldwide to treat the coronavirus disease (COVID-19). Part I: Complexation with iodine in different solvents, J. Mol. Liq. 325 (2021) 115187.

[38] A.M.A. Adam, M.S. Refat, T.A. Altalhi, F.S. Aldawsari, Charge-transfer (CT) dynamics of triamterene with 2,3-dichloro-5, 6-dicyano-p-benzoquinone acceptor: A $n\rightarrow\pi^*$ model CT complex generated by liquid- and solid-state reactions, J. Mol. Liq. 334 (2021) 116119.

[39] A.M.A. Adam, T.A. Altalhi, H.A. Saad, A.M. Alsuhaibani, M.S. Refat, M.S. Hegab, Correlations between spectroscopic data for charge-transfer complexes of two artificial sweeteners, aspartame and neotame, generated with several π-acceptors, J. Mol. Liq. 334 (2021) 115904.

[40] A.M.A. Adam, T.A. Altalhi, H.A. Saad, M.S. Refat, M.S. Hegab, Exploring the charge-transfer chemistry of fluorine-containing pyrazolin-5-ones: The complexation of 1-methyl-3-trifluoromethyl-2-pyrazoline-5-one with five π-acceptors, J. Mol. Liq. 331 (2021) 115814.

[41] A.M.A. Adam, M.S. Refat, A comparison of charge-transfer complexes of iodine with some antibiotics formed through two different approaches (liquid-liquid vs solid-solid), J. Mol. Liq. 329 (2021) 115560.

[42] R.M. Alghanmi, M.T. Basha, S.M. Soliman, R.K. Alsaeedi, Synthesis, and spectroscopic, nanostructure, surface morphology, and density functional theory studies of new charge-transfer complexes of amifampridine with π-acceptors, J. Mol. Liq. 326 (2021) 115199.

[43] Ola A.El-Gammal, Ashraf A. El-Bindary, Farid Sh. Mohamed, Ghada N. Rezk, Mohamed A. El-Bindary, Synthesis, characterization, design, molecular docking, anti COVID-19 activity, DFT calculations of novel Schiff base with some transition metal complexes, J. Mol. Liq. 330 (2022) 115522.

[44] X. Luo, W. Shi, Y. Yang, Y. Li, Fluorescence probes detecting $O_2\bullet$ based on intramolecular charge transfer and excited-state intramolecular proton transfer mechanisms, J. Mol. Liq. 322 (2021) 114886.

[45] S. Halder, R. Aggrawal, V.K. Aswal, D. Ray, S.K. Saha, Study of refolding of a denatured protein and microenvironment probed through FRET to a twisted intramolecular charge transfer fluorescent biosensor molecule, J. Mol. Liq. 322 (2021) 114532.

[46] I.M. Khan, K. Alam, M.J. Alam, Exploring charge transfer dynamics and photocatalytic behavior of designed donor-acceptor complex: Characterization, spectrophotometric and theoretical studies (DFT/TD-DFT), J. Mol. Liq. 310 (2020) 113213.

[47] M.T. Basha, R.M. Alghanmi, S.M. Soliman, W.J. Alharby, Synthesis, spectroscopic, thermal, structural characterization and DFT/TD-DFT computational studies for charge transfer complexes of 2,4-diamino pyrimidine with some benzoquinone acceptors, J. Mol. Liq. 309 (2020) 113210.

[48] X. Li, Z. Lai, J. Gu, W. Liu, J. Gao, Q. Wang, Sequential determination of cerium (IV) ion and ascorbic acid via a novel organic framework: A subtle interplay between intramolecular charge transfer (ICT) and aggregated-induced-emission (AIE), J. Mol. Liq. 304 (2020) 112705.

[49] T.A. Altalhi, Utilization of tannic acid into spherical structured carbons based on charge-transfer complexation with tetracyanoethylene acceptor: Liquid-liquid and solid-solid interactions, J. Mol. Liq. 300 (2020) 112325.

[50] A. Karmakar, P. Bandyopadhyay, S. Banerjee, N.C. Mandal, B. Singh, Synthesis, spectroscopic, theoretical and antimicrobial studies on molecular charge-transfer complex of 4-(2-thiazolylazo)resorcinol (TAR) with 3, 5-dinitrosalicylic acid, picric acid, and chloranilic acid, J. Mol. Liq. 299 (2020) 112217.

[51] F.A. Al-Saif, A.A. El-Habeeb, M.S. Refat, H.H. Eldaroti, A.M.A. Adam, H. Fetooh, H.A. Saad, Chemical and physical properties of the charge transfer complexes of domperidone antiemetic agent with π-acceptors, J. Mol. Liq. 293 (2019) 111517.

[52] F.A. Al-Saif, A.A. El-Habeeb, M.S. Refat, A.M.A. Adam, H.A. Saad, A.I. El-Shenawy, H. Fetooh, Characterization of charge transfer products obtained from the reaction of the sedative-hypnotic drug barbital with chloranilic acid, chloranil, TCNQ and DBQ organic acceptors, J. Mol. Liq. 287 (2019) 110981.

[53] H. AlRabiah, H.A. Abdel-Aziz, G.A.E. Mostafa, Charge transfer complexes of brucine with chloranilic acid, 2,3-dichloro-5,6-dicyano-1,4-benzoquinone and tetracyanoquinodimethane: Synthesis, spectroscopic characterization and antimicrobial activity, J. Mol. Liq. 286 (2019) 110754.

[54] S. Khopkar, M. Jachak, G. Shankarling, Viscosity sensitive semisquaraines based on 1, 1, 2-trimethyl-1H-benzo[*e*]indole: Photophysical properties, intramolecular charge transfer, solvatochromism, electrochemical and DFT study, J. Mol. Liq. 285 (2019) 123–135.

[55] A. Mostafa, S. Madrahimov, J. Fadlallah, S.Y. AlQaradawi, UV–Vis, IR spectra, mass spectrometry and thermal studies of charge transfer complexes formed in the reaction of 1, 4, 8, 11-tetraazacyclotetradecane with π-electron acceptors, J. Mol. Liq. 284 (2019) 616–624.

[56] K.M. Al-Ahmary, M.M. Habeeb, S.H. Aljahdali, Synthesis, spectroscopic studies and DFT/TD-DFT/PCM calculations of molecular structure, spectroscopic characterization and NBO of charge transfer complex between 5-amino-1,3-dimethylpyrazole (5-ADMP) with chloranilic acid (CLA) in different solvents, J. Mol. Liq. 277 (2019) 453–470.
[57] L. Miyan, A. Zulkarnain, Ahmad, Spectroscopic and spectrophotometric studies on hydrogen bonded charge transfer complex of 2-amino-4-methylthiazole with chloranilic acid at different temperatures, J. Mol. Liq. 262 (2018) 514–526.
[58] A.S.A. Almalki, A. Alhadhrami, R.J. Obaid, M.A. Alsharif, A.M.A. Adam, I. Grabchev, M.S. Refat, Preparation of some compounds and study their thermal stability for use in dye sensitized solar cells, J. Mol. Liq. 261 (2018) 565–582.
[59] M.A. El-Bindary, M.G. El-Desouky, A.A. El-Bindary, Metal–organic frameworks encapsulated with an anticancer compound as drug delivery system: Synthesis, characterization, antioxidant, anticancer, antibacterial, and molecular docking investigation, Appl. Organomet. Chem. 36 (5) (2022) e6660.
[60] O.R. Shehab, H. AlRabiah, H.A. Abdel-Aziz, G.A.E. Mostafa, Charge-transfer complexes of cefpodoxime proxetil with chloranilic acid and 2,3-dichloro-5,6-dicyano-1,4-benzoquinone: Experimental and theoretical studies, J. Mol. Liq. 257 (2018) 42–51.
[61] R.M. Alghanmi, S.M. Soliman, M.T. Basha, M.M. Habeeb, Electronic spectral studies and DFT computational analysis of hydrogen bonded charge transfer complexes between chloranilic acid and 2,5-dihydroxy-p-benzoquinone with 2-amino-4-methylbenzothiazole in methanol, J. Mol. Liq. 256 (2018) 433–444.
[62] I.M. Khan, S. Shakya, N. Singh, Preparation, single-crystal investigation and spectrophotometric studies of proton transfer complex of 2,6-diaminopyridine with oxalic acid in various polar solvents, J. Mol. Liq. 250 (2018) 150–161.
[63] A. Karmakar, B. Singh, Charge-transfer complex of 1-(2-Thiazolylazo)-2-naphthol with aromatic nitro compounds: Experimental and theoretical studies, J. Mol. Liq. 247 (2017) 425–433.
[64] M. Zhang, M. Zhang, Y. Liu, Y. Chen, K. Zhang, C. Wang, X. Zhao, C. Zhou, J. Gao, X. Xie, D. Zheng, G. Zhao, DFT/TDDFT theoretical investigation on the excited-state intermolecular hydrogen bonding interactions, photoinduced charge transfer, and vibrational spectroscopic properties of deprotonated deoxyadenosine monophosphate [dAMP-H]− anion in aqueous solution: Upon photoexcitation of hydrogen-bonded model complexes [dAMP-H]−nH_2O (n = 0, 1, 2, 3, 4), J. Mol. Liq. 242 (2017) 1118–1122.
[65] A. Karmakar, B. Singh, Charge-transfer interaction of 4-(2-pyridylazo) resorcinol with nitroaromatics: Insights from experimental and theoretical result, J. Mol. Liq. 236 (2017) 135–143.
[66] A.S.A. Almalki, A.M. Naglah, M.S. Refat, M.S. Hegab, A.M.A. Adam, M.A. Al-Omar, Liquid and solid-state study of antioxidant quercetin donor and TCNE acceptor interaction: Focusing on solvent affect on the morphological properties, J. Mol. Liq. 233 (2017) 292–302.
[67] K.M. Al-Ahmary, S.M. Soliman, R.A. Mekheimer, M.M. Habeeb, M.S. Alenezi, Synthesis, spectral studies and DFT computational analysis of hydrogen bonded-charge transfer complex between chloranilic acid with 2,4-diamino-quinoline-3-carbonitrile in different polar solvents, J. Mol. Liq. 231 (2017) 602–619.
[68] L. Miyan, S. Qamar, A. Ahmad, Synthesis, characterization and spectrophotometric studies of charge transfer interaction between donor imidazole and π acceptor 2,4-dinitro-1-naphthol in various polar solvents, J. Mol. Liq. 225 (2017) 713–722.
[69] A.M.A. Adam, M.S. Refat, M.S. Hegab, H.A. Saad, Spectrophotometric and thermodynamic studies on the 1:1 charge transfer interaction of several clinically important drugs with tetracyanoethylene in solution-state: Part one, J. Mol. Liq. 224 (2016) 311–321.
[70] L. Abdelmalek, M. Fatiha, N. Leila, C. Mouna, M. Nora, K. Djameleddine, Computational study of inclusion complex formation between carvacrol and β-cyclodextrin in vacuum and in water: Charge transfer, electronic transitions and NBO analysis, J. Mol. Liq. 224 (2016) 62–71.
[71] K.R. Mahmoud, M.S. Refat, T. Sharshar, A.M.A. Adam, E.A. Manaaa, Synthesis of amino acid iodine charge transfer complexes *in situ* methanolic medium: Chemical and physical investigations, J. Mol. Liq. 222 (2016) 1061–1067.
[72] N. Rahman, S. Sameen, M. Kashif, Spectroscopic study of charge transfer complexation between doxepin and π–acceptors and its application in quantitative analysis, J. Mol. Liq. 222 (2016) 944–952.
[73] N. Singh, I.M. Khan, A. Ahmad, S. Javed, Synthesis, spectrophotometric and thermodynamic studies of charge transfer complex of 5,6-dimethylbenzimidazole with chloranilic acid at various temperatures in acetonitrile and methanol solvents, J. Mol. Liq. 221 (2016) 1111–1120.
[74] K.M. Al-Ahmary, M.S. Alenezi, M.M. Habeeb, Synthesis, spectroscopic and DFT theoretical studies on the hydrogen bonded charge transfer complex of 4-aminoquinoline with chloranilic acid, J. Mol. Liq. 220 (2016) 166–182.
[75] L. Miyan, A. Ahmad, Synthesis, spectroscopic and spectrophotometric studies of charge transfer complex of the donor 3,4-diaminotoluene with π-acceptor 2,3-dichloro-5,6-dicyano-*p*-benzoquinone in different polar solvents, J. Mol. Liq. 219 (2016) 614–623.
[76] A.M.A. Adam, M.S. Refat, Solution and solid-state investigations of charge transfer complexes caused by the interaction of bathophenanthroline with different organic acceptors in a (methanol + dichloromethane) binary solvent system, J. Mol. Liq. 219 (2016) 377–389.
[77] A.M.A. Adam, M.S. Refat, H.A. Saad, M.S. Hegab, Charge transfer complexation of the anticholinergic drug clidinium bromide and picric acid in different polar solvents: Solvent effect on the spectroscopic and structural morphology properties of the product, J. Mol. Liq. 216 (2016) 192–208.
[78] H.S. El-Sheshtawy, M.M. Ibrahim, M.R.E. Aly, M. El-Kemary, Spectroscopic and structure investigation of the molecular complexes of tris(2-aminoethyl) amine with π-acceptors, J. Mol. Liq. 213 (2016) 82–91.
[79] A.S. Al-Attas, D.S. Al-Raimi, M.M. Habeeb, Spectroscopic analysis, thermodynamic study and molecular modeling of charge transfer complexation between 2-amino-5,6-dimethyl-1,2,4-triazine with DDQ in acetonitrile, J. Mol. Liq. 198 (2014) 114–121.
[80] R. Kumar, A.J.A. Baskar, V. Kannappan, D. RoopSingh, Acoustical and spectroscopic investigation of charge transfer complexes of certain aromatic compounds with iodine in n-hexane at 303 K, J. Mol. Liq. 196 (2014) 404–410.
[81] N. Singh, I.M. Khan, A. Ahmad, S. Javed, Synthesis, crystallographic and spectrophotometric studies of charge transfer complex formed between 2,2′-bipyridine and 3,5-dinitrosalicylic acid, J. Mol. Liq. 191 (2014) 142–150.
[82] R.M. Alghanmi, M.M. Habeeb, Spectral and solvation effect studies on charge transfer complex of 2, 6-diaminopyridine with chloranilic acid, J. Mol. Liq. 181 (2013) 20–28.
[83] R. Kumar, G. Padmanabhan, V. Ulagendran, V. Kannappan, S. Jayakumar, Ultrasonic and optical studies on charge transfer complexes of p-chloranil with certain aromatic hydrocarbons in DMSO at 303.15 K, J. Mol. Liq. 162 (2011) 141–147.
[84] K.M. Al-Ahmary, M.M. Habeeb, E.A. Al-Solmy, Spectroscopic studies of the hydrogen bonded charge transfer complex of 2-aminopyridine with π-acceptor chloranilic acid in different polar solvents, J. Mol. Liq. 162 (2011) 129–134.
[85] V. Ulagendran, R. Kumar, S. Jayakumar, V. Kannappan, Ultrasonic and spectroscopic investigations of charge-transfer complexes in ternary liquid mixtures, J. Mol. Liq. 148 (2–3) (2009) 67–72.
[86] E.H. EL-Mossalamy, Molecular spectroscopic studies of charge transfer complexes of thiourea derivatives with benzoquinones, J. Mol. Liq. 123 (2–3) (2006) 118-123.
[87] Ghaferah H. Al-Hazmi, A.M. Hassanien, A.A. Atta, Moamen S. Refat, Hosam A. Saad, Sonam Shakya, Abdel Majid A. Adam, Supramolecular charge-transfer complex generated by the interaction between tin(II) 2,3-naphtalocyanine as a donor with DDQ as an acceptor: Spectroscopic studies in solution state and theoretical calculations, J. Mol. Liq. (2022) 119757.
[88] A.M.A. Adam, M.S. Hegab, M.S. Refat, H.H. Eldaroti, Proton-transfer and charge-transfer interactions between the antibiotic trimethoprim and several σ- and π- acceptors: A spectroscopic study, J. Mol. Struct. 1231 (2020) 129687.
[89] A.M.A. Adam, H.H. Eldaroti, M.S. Hegab, M.S. Refat, J.Y. Al-Humaidi, H.A. Saad, Measurements and correlations in solution-state for charge transfer products caused from the 1:2 complexation of TCNE acceptor with several important drugs, Spectrochim. Acta A 211 (2019) 166–177.
[90] O.B. Ibrahim, E.A. Manaaa, M.M. AL-Majthoub, A.M. Fallatah, A.M.A. Adam, M. M. Alatibi, J.Y. Al-Humaidi, M.S. Refat, Estimation of metformin drug for the diabetes patients by simple, quick and cheap techniques within the formation of colored charge transfer complexes, Spectrosc. Spect. Anal. 38 (11) (2018) 3622-3630.
[91] M.S. Refat, A.M.A. Adam, M.Y. El-Sayed, Biomarkers charge-transfer complexes of melamine with quinol and picric acid: Synthesis, spectroscopic, thermal, kinetic and biological studies, Arabian J. Chem. 10 (2017) S3482.
[92] A.M.A. Adam, M.S. Refat, H.A. Saad, Quick and simple formation of different nanosized charge-transfer complexes of the antibiotic drug moxifloxacin: An efficient way to remove and utilize discarded antibiotics, C.R. Chimie 18 (2015) 914–928.
[93] A.M.A. Adam, M.S. Refat, H.A. Saad, M.S. Hegab, An environmentally friendly method to remove and utilize the highly toxic strychnine in other products based on proton-transfer complexation, J. Mol. Struct. 1102 (2015) 170–185.
[94] M.S. Refat, A.M.A. Adam, H.A. Saad, Utility of charge-transfer complexation for the assessment of macrocyclic polyethers: Spectroscopic, thermal and surface morphology characteristics of two highly crown ethers complexed with acido acceptors, J. Mol. Strutct. 1085 (2015) 178–190.
[95] M.S. Refat, H.A. Saad, A.M.A. Adam, Spectral, thermal and kinetic studies of charge-transfer complexes formed between the highly effective antibiotic drug metronidazole and two types of acceptors: σ- and π-acceptors, Spectrochim. Acta A 141 (2015) 202–210.
[96] M.S. Refat, L.A. Ismail, A.M.A. Adam, Shedding light on the photostability of two intermolecular charge-transfer complexes between highly fluorescent bis-1, 8-naphthalimide dyes and some p-acceptors: A spectroscopic study in solution and solid states, Spectrochim. Acta A 134 (2015) 288–301.
[97] M.S. Refat, H.A. Saad, A.M.A. Adam, H.H. Eldaroti, A Structural Study of the Intermolecular Interactions of Tyramine with Some π-Acceptors: Quantification of Biogenic Amines Based on Charge-Transfer Complexation, J. Gen. Chem. 85 (1) (2015) 181–191.
[98] M.S. Refat, A.M.A. Adam, H.A. Saad, A.M. Naglah, M.A. Al-Omar, Charge–transfer Complexation and Photostability Characteristics of Iodine with bis-1,8-naphthalimide as a Photosensitive Biologically Active Units in Solution and in the Solid State: Linear Correlation of Photostability and Dissociation Energy, Int. J. Electrochem. Sci. 10 (2015) 6405–6421.

[99] O.B. Ibrahim, M.M. AL-Majthoub, M.A. Mohamed, A.M.A. Ada, M.S. Refat, Quick and Simple Formation of Charge Transfer Complexes of Brain and Nerves Phenytoin Drug with Different π–acceptors: Chemical and Biological Studies, Int. J. Electrochem. Sci. 10 (2015) 1065-1080.
[100] A.M.A. Adam, M.S. Refat, Chemistry of drug interactions: Characterization of charge-transfer complexes of Guaifenesin with various acceptors using spectroscopic and thermal methods, J. Gen. Chem. 84 (9) (2014) 1847–1856.
[101] M.S. Refat, H.A. Saad, A.M.A. Adam, Infrared, Raman, ^{1}H NMR, TG, and SEM Properties of the Charge-Transfer Interactions between Tris(hydroxymethyl) methane with the Acceptors Picric Acid, Chloranilic Acid, and 1,3-Dinitrobenzene, J. Gen. Chem. 84 (7) (2014) 1417–1428.
[102] A.M.A. Adam, Application of Charge-Transfer Complexation for Evaluation of the Drug-Receptor Mechanism of Interaction: Spectroscopic and Structure Morphological Properties of Procaine and Pilocarpine Complexes with Chloranilic Acid Acceptor, J. Gen. Chem. 84 (6) (2014) 1225–1236.
[103] A.M.A. Adam, Nano-structured complexes of reserpine and quinidine drugs with chloranilic acid based on intermolecular H-bond: Spectral and surface morphology studies, Spectrochim. Acta A 127 (2014) 107–114.
[104] M.S. Refat, A.M.A. Adam, T. Sharshar, H.A. Saad, H.H. Eldaroti, Utility of positron annihilation lifetime technique for the assessment of spectroscopic data of some charge-transfer complexes derived from N-(1-Naphthyl) ethylenediamine dihydrochloride, Spectrochim. Acta A 122 (2014) 34–47.
[105] H.H. Eldaroti, S.A. Gadir, M.S. Refat, A.M.A. Adam, Charge-transfer interaction of drug quinidine with quinol, picric acid and DDQ: Spectroscopic characterization and biological activity studies towards understanding the drug–receptor mechanism, J. Pharm. Anal. 4 (2) (2014) 81–95.
[106] M.S. Refat, O.B. Ibrahim, H.A. Saad, A.M.A. Adam, Usefulness of charge–transfer complexation for the assessment of sympathomimetic drugs: Spectroscopic properties of drug ephedrine hydrochloride complexed with some p-acceptors, J. Mol. Struct. 1064 (2014) 58–69.
[107] H.H. Eldaroti, S.A. Gadir, M.S. Refat, A.M.A. Adam, Spectroscopic investigations of the charge-transfer interaction between the drug reserpine and different acceptors: Towards understanding of drug–receptor mechanism, Spectrochim. Acta A 115 (2013) 309–323.
[108] H.H. Eldaroti, S.A. Gadir, M.S. Refat, A.M.A. Adam, Preparation, spectroscopic and thermal characterization of new charge-transfer complexes of ethidium bromide with π-acceptors. In vitro biological activity studies, Spectrochim. Acta A 109 (2013) 259–271.
[109] A.M.A. Adam, Structural, thermal, morphological and biological studies of proton-transfer complexes formed from 4-aminoantipyrine with quinol and picric acid, Spectrochim. Acta A 104 (2013) 1–13.
[110] A.M.A. Adam, M.S. Refat, H.A. Saad, Spectral, thermal, XRD and SEM studies of charge-transfer complexation of hexamethylenediamine and three types of acceptors: π-, σ- and vacant orbital acceptors that include quinol, picric acid, bromine, iodine, $SnCl_4$ and $ZnCl_2$ acceptors, J. Mol. Struct. 1051 (2013) 144–163.
[111] A.M.A. Adam, M.S. Refat, H.A. Saad, Utilization of charge-transfer complexation for the detection of carcinogenic substances in foods: Spectroscopic characterization of ethyl carbamate with some traditional π-acceptors, J. Mol. Strut. 1037 (2013) 376–392.
[112] H.H. Eldaroti, S.A. Gadir, M.S. Refat, A.M.A. Adam, Charge transfer complexes of the donor acriflavine and the acceptors quinol, picric acid, TCNQ and DDQ: Synthesis, spectroscopic characterizations and antimicrobial studies, Int. J. Electrochem. Sci. 8 (2013) 5774–5800.
[113] A.M.A. Adam, Synthesis, spectroscopic, thermal and antimicrobial investigations of charge-transfer complexes formed from the drug procaine hydrochloride with quinol, picric acid and TCNQ, J. Mol. Struct. 1030 (2012) 26–39.
[114] A.M.A. Adam, M.S. Refat, T. Sharshar, Z.K. Heiba, Synthesis and characterization of highly conductive charge-transfer complexes using positron annihilation spectroscopy, Spectrochim. Acta A 95 (2012) 458–477.
[115] M.S. Refat, H.A. Saad, A.M.A. Adam, Intermolecular hydrogen bond complexes by in situ charge transfer complexation of o-tolidine with picric and chloranilic acids, Spectrochim. Acta A 79 (2011) 672–679.
[116] M.S. Refat, H.A. Saad, A.M.A. Adam, Proton transfer complexes based on some π-acceptors having acidic protons with 3-amino-6-[2-(2-thienyl)vinyl]-1,2,4-triazin-5(4*H*)-one donor: Synthesis and spectroscopic characterizations, J. Mol. Struct. 995 (1–3) (2011) 116–124.
[117] A.M.A. Adam, M.S. Refat, Analysis of charge-transfer complexes caused by the interaction of the antihypertensive drug valsartan with several acceptors in CH_2Cl_2 and $CHCl_3$ solvents and correlations between their spectroscopic parameters, J. Mol. Liq. 348 (2022) 118466.
[118] A.M.A. Adam, H.A. Saad, M.S. Refat, M.S. Hegab, Charge-transfer complexes of antipsychotic drug sulpiride with inorganic and organic acceptors generated through two different approaches: Spectral characterization, J. Mol. Liq. 353 (2022) 118819.
[119] A.M.A. Adam, H.A. Saad, A.A. Atta, M. Alsawat, M.S. Hegab, M.S. Refat, T.A. Altalhi, E.H. Alosaimi, A.A.O. Younes, Usefulness of charge-transfer interaction between urea and vacant *orbital* acceptors to generate novel adsorbent material for the adsorption of pesticides from irrigation water, J. Mol. Liq. 349 (2022) 118188.
[120] A.M.A. Adam, H.A. Saad, A.A. Atta, M. Alsawat, M.S. Hegab, T.A. Altalhi, M.S. Refat, An Environmentally Friendly Method for Removing Hg(II), Pb(II), Cd(II) and Sn(II) Heavy Metals from Wastewater Using Novel Metal–Carbon-Based Composites, Crystals 11 (2021) 882, https://doi.org/10.3390/cryst11080882.
[121] A.M.A. Adam, H.A. Saad, A.A. Atta, M. Alsawat, M.S. Hegab, M.S. Refat, T.A. Altalhi, E.H. Alosaimi, A.A.O. Younes, Preparation and Characterization of New CrFeO3-Carbon Composite Using Environmentally Friendly Methods to Remove Organic Dye Pollutants from Aqueous Solutions, Crystals 11 (2021) 960, https://doi.org/10.3390/cryst11080960.
[122] A.M.A. Adam, H.A. Saad, M.S. Refat, M.S. Hegab, Charge-transfer chemistry of two corticosteroids used adjunctively to treat COVID-19. Part I: Complexation of hydrocortisone and dexamethasone donors with DDQ acceptor in five organic solvents, J. Mol. Liq. 357 (2022) 119092.
[123] J. Tauc, R. Grigorovici, A. Vancu, Optical Properties and Electronic Structure of Amorphous Germanium, Phys. Status Solidi B 15 (2) (1966) 627–637, https://doi.org/10.1002/pssb.19660150224.
[124] E.A. Davis, N.F. Mott, Conduction in non-crystalline systems V. Conductivity, optical absorption and photoconductivity in amorphous semiconductors, Philosophical Magazine 22 (179) (1970) 903–922, https://doi.org/10.1080/14786437008221061.
[125] N.F. Mott, E.A. Davis, Electrochemical Process in Non-crystalline Materials, Calendron Press, Oxford, 1979.
[126] H.A. Benesi, J.H. Hildebrand, A Spectrophotometric Investigation of the Interaction of Iodine with Aromatic Hydrocarbons, J. Am. Chem. Soc. 71 (8) (1949) 2703–2707.
[127] A.B.P. Lever, Inorganic Electronic Spectroscopy, second ed., Elsevier, Amsterdam, 1985.
[128] H. Tsubumora, R. Lang, Molecular complexes and their spectra. XIII. complexes of iodine with amides, diethyl sulfide and diethyl disulfide, J. Am. Chem. Soc. 83 (9) (1961) 2085–2092.
[129] A. Alagha, A. Nourallah, S. Hariri, Characterization of dexamethasone loaded collagen-chitosan sponge and in vitro release study, J. Drug Deliv. Sci. Technol. 55 (2020) 101449.
[130] A. Sanjana, M.G. Ahmed, J. Gowda Bh, Preparation and evaluation of in-situ gels containing hydrocortisone for the treatment of aphthous ulcer, J. Oral Biol. Craniofac. Res. 11 (2) (2021) 269–276.
[131] S. Soumya, I. Hubert Joe, A combined experimental and quantum chemical study on molecular structure, spectroscopic properties and biological activity of anti-inflammatory Glucocorticosteroid drug, Dexamethasone, J. Mol. Struct. 1245 (2021) 130999.